

CONSTRUCTION AND SHARP CONSISTENCY ESTIMATES FOR ATOMISTIC/CONTINUUM COUPLING METHODS WITH GENERAL INTERFACES: A 2D MODEL PROBLEM

C. ORTNER AND L. ZHANG

ABSTRACT. We present a new variant of the geometry reconstruction approach for the formulation of atomistic/continuum coupling methods (a/c methods). For multi-body nearest-neighbour interactions on the 2D triangular lattice, we show that patch test consistent a/c methods can be constructed for arbitrary interface geometries. Moreover, we prove that all methods within this class are first-order consistent at the atomistic/continuum interface and second-order consistent in the interior of the continuum region.

1. INTRODUCTION

Atomistic/continuum coupling methods (a/c methods) are a class of coarse-graining techniques for the efficient simulation of atomistic systems with localized regions of interest interacting with long-range elastic effects that can be adequately described by a continuum model. We refer to [6], and references therein, for an introduction and discussion of applications.

In the present work we are concerned with the construction and rigorous analysis of energy-based a/c methods in a 2D model problem. Our starting point is the geometry reconstruction approach proposed by Shimokawa *et al* [17] and by E, Lu and Yang [3] for the construction of “consistent” a/c methods in 2D and 3D. We propose a new variant of that approach to define a modified site potential at the a/c interface, which has several free parameters. We then “fit” these parameters so that the resulting a/c hybrid energy satisfies an energy consistency condition and a force consistency condition (see (2.6) and (2.7) for the precise definition of these terms; in the terminology of quasicontinuum methods our hybrid energy is free of ghost forces).

Explicit constructions along these lines can be found in [17] for pair potentials and in [3] for coupling a finite-range multi-body potential to a nearest-neighbour potential, for high-symmetry interfaces. Our focus in the present work is the coupling to a continuum model and interfaces with corners; both of these cases are only briefly touched upon in [3].

In recent years there has been considerable activity in the numerical analysis literature on the classification and rigorous analysis of a/c methods (see [1, 2, 7, 10, 12] and references therein). Much of this work has been restricted to one-dimensional problems; only very recently some progress has been made on the analysis of a/c methods in 2D and 3D [5, 9, 11].

The first rigorous error estimates for the method proposed in [3] (together with a wider class of related methods), in more than one dimension, are presented in [9] for 2D finite range

Date: November 15, 2018.

2000 Mathematics Subject Classification. 65N12, 65N15, 70C20.

Key words and phrases. atomistic models, quasicontinuum method, coarse graining.

This work was supported by EPSRC Grant “Analysis of Atomistic-to-Continuum Coupling Methods” and the EPSRC Critical Mass Programme “New Frontiers in the Mathematics of Solids” (OxMoS)..

multi-body interactions. The work [9] *assumes* the existence of an interface potential so that the resulting a/c energy satisfies certain energy and force consistency conditions (a variant of the *patch test*) and then established first-order consistency of the resulting a/c method in negative Sobolev norms.

Several important questions remain open: 1. It is yet unclear whether constructions of the type proposed in [3, 17] can be carried out for interfaces with corners. 2. The error estimates in [9] contain certain non-local terms that enforce unnatural assumptions (e.g., connectedness of the atomistic region). 3. Moreover, this nonlocality causes suboptimal error estimates; namely, it destroys the second-order consistency of the Cauchy–Born model (see, e.g., [1, 4, 10]), and an unnatural dependence of the interface width enters the error estimates. (Moreover, we note that the error estimates in [11] for a different a/c method are only first-order as well.)

The purpose of the present work is to investigate for a model problem whether these restrictions are genuine, or of a technical nature. To that end we formulate an atomistic model on the 2D triangular lattice with nearest-neighbour multi-body interactions (effectively these are third neighbour interactions), and construct new a/c methods in the spirit of [3, 17]. We then prove that the resulting methods are all first-order consistent in the interface region and second-order consistent in the interior of the continuum region, which is the first generalisation of the optimal one-dimensional result [10, Theorem 3.1] to two dimensions.

Although it may seem restrictive at first glance to consider only nearest-neighbour potentials, we note that this is in fact an important case to consider. For example, bond-angle potentials (which are included in our analysis) usually consider only angles between nearest-neighbour bonds. More generally, multi-body effects are usually restricted to very small interaction neighbourhoods, while long-range effects are often only displayed in pair potentials (in particular, Lennard-Jones and Coulomb), which can be treated, for example, using Shapeev’s method [11, 15, 14].

2. ATOMISTIC CONTINUUM COUPLING

2.1. Atomistic model. We consider a nominally infinite crystal, but restrict admissible displacements to those with compact support. Thus we avoid any discussion of boundary conditions, which are unimportant for the purpose of this work.

Let \mathbf{Q}_6 denote a rotation through arclength $\pi/3$. As a reference configuration we choose the triangular lattice (see also Figure 1):

$$\begin{aligned} \mathcal{L} &:= \mathbf{A}\mathbb{Z}^2, & \text{where } \mathbf{A} &:= (a_1, a_2), \\ & & a_1 &:= (1, 0)^\top, \text{ and } a_j := \mathbf{Q}_6^{j-1}a_1, j \in \mathbb{Z}. \end{aligned}$$

We will frequently use the following relationships between the vectors a_j :

$$a_{j+6} = a_j, \quad a_{j+3} = -a_j, \quad \text{and} \quad a_{j-1} + a_{j+1} = a_j \quad \text{for all } j \in \mathbb{Z}.$$

For future reference we also define $\mathbf{a} := (a_j)_{j=1}^6$, and $\mathbf{F}\mathbf{a} := (\mathbf{F}a_j)_{j=1}^6$, for $\mathbf{F} \in \mathbb{R}^{2 \times 2}$.

Our choice of reference configuration is largely motivated by the fact that \mathcal{L} possesses a canonical triangulation (see Figure 1, and §2.2), which will be convenient in our analysis.

The set of displacements and deformations with compact support are given, respectively, by

$$\begin{aligned} \mathcal{U}_0 &:= \{u : \mathcal{L} \rightarrow \mathbb{R}^2 : u(x) \neq 0 \text{ for at most finitely many } x \in \mathcal{L}\}, & \text{and} \\ \mathcal{Y}_0 &:= \{y : \mathcal{L} \rightarrow \mathbb{R}^2 : y - \text{id} \in \mathcal{U}_0\}. \end{aligned}$$

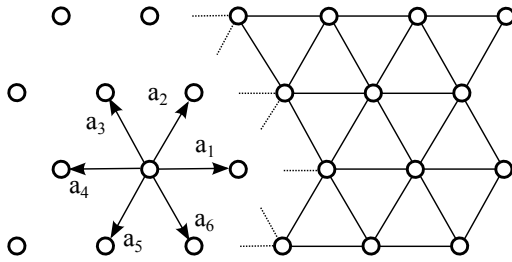


FIGURE 1. The 2D triangular lattice and its canonical triangulation.

We remark that deformations are usually required to be at least invertible, but that we avoid this requirement by making simplifying assumptions on the interaction potential.

A homogeneous deformation is a map $y_F : \mathcal{L} \rightarrow \mathbb{R}^2$, $y_F(x) := Fx$, where $F \in \mathbb{R}^{2 \times 2}$. We note that $y_F \notin \mathcal{Y}_0$ unless $F = I$.

For a map $v : \mathcal{L} \rightarrow \mathbb{R}^k$, $k \in \mathbb{N}$, we define the forward finite difference operator

$$D_j v(x) := v(x + a_j) - v(x), \quad x \in \mathcal{L}, j \in \mathbb{Z},$$

and we define the family of all nearest-neighbour finite differences as $Dy(x) := (D_j y(x))_{j=1}^6$.

We assume that the atomistic interaction is described by a nearest-neighbour multi-body site energy potential $V \in C^3(\mathbb{R}^{2 \times 6})$, with $V(\mathbf{a}) = 0$, so that the energy of a deformation $y \in \mathcal{Y}_0$ is given by

$$\mathcal{E}_a(y) := \sum_{x \in \mathcal{L}} V(Dy(x)).$$

The assumption $V(\mathbf{a}) = 0$ guarantees that $\mathcal{E}_a(y)$ is finite for all $y \in \mathcal{Y}_0$.

2.2. The Cauchy–Born approximation. For deformation fields $y \in W^{1,\infty}(\mathbb{R}^2; \mathbb{R}^2)$, such that $y - \text{id}$ has compact support, we define the Cauchy–Born energy functional

$$\mathcal{E}_c(y) := \int_{\mathbb{R}^2} W(\partial y) dx, \quad \text{where } W(F) := \frac{1}{\Omega_0} V(\mathbf{F}\mathbf{a}),$$

$W \in C^3(\mathbb{R}^{2 \times 2}; \mathbb{R})$, is the *Cauchy–Born stored energy function*. The factor $\Omega_0 := \sqrt{3}/2$ is the volume of one primitive cell of \mathcal{L} , that is, $W(F)$ is the energy per unit volume of the lattice $F\mathcal{L}$.

If $y \in \mathcal{Y}_0$ is a *discrete* deformation, then we define its Cauchy–Born energy through piecewise affine interpolation: The triangular lattice \mathcal{L} has a canonical triangulation \mathcal{T} into closed triangles depicted in Figure 1. Henceforth, we shall always identify a function $v : \mathcal{L} \rightarrow \mathbb{R}^k$ with its P_1 -interpolant, which belongs to $W^{1,\infty}(\mathbb{R}^2; \mathbb{R}^k)$. For a discrete deformation $y \in \mathcal{Y}_0$, we can then write the Cauchy–Born energy as

$$\mathcal{E}_c(y) = \int_{\mathbb{R}^2} W(\partial y) dx = \sum_{T \in \mathcal{T}} |T| W(\partial_T y), \quad (2.1)$$

where we define $\partial_T y := \partial y(x)|_{x \in T}$ and note that $|T| = \Omega_0/2$ for all triangles $T \in \mathcal{T}$.

Note that $W(I) = 0$ and hence $\mathcal{E}_c(y)$ is finite for all $y \in \mathcal{Y}_0$.

Alternatively, \mathcal{E}_c can be written in terms of site energies, which will be helpful for the definition of a/c methods. Each vertex $x \in \mathcal{L}$ has six adjacent triangles, which we denote by

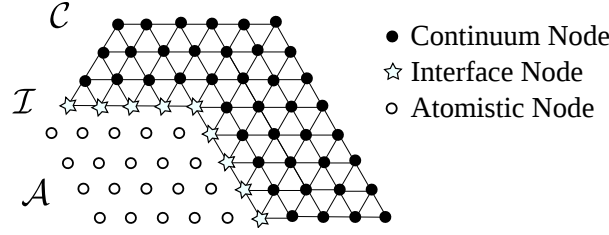


FIGURE 2. Atomistic-interface-continuum domain decomposition.

$T_{x,j} := \text{conv}\{x, x + a_j, x + a_{j+1}\}$, $j = 1, \dots, 6$ (cf. Figure 3). With this notation,

$$\mathcal{E}_c(y) = \sum_{x \in \mathcal{L}} V^c(Dy(x)), \quad \text{where} \quad V^c(Dy(x)) := \frac{\Omega_0}{6} \sum_{j=1}^6 W(\partial_{T_{x,j}} y). \quad (2.2)$$

Note that $V^c \in C^3(\mathbb{R}^{2 \times 6})$ is well-defined since $\partial_{T_{x,j}} y$ is determined by the finite differences $D_j y(x)$ and $D_{j+1} y(x)$.

2.3. A/c coupling via geometry reconstruction. Let $\mathcal{A} \subset \mathcal{L}$ denote the set of all lattice sites for which we require full atomistic accuracy. We denote the set of interface lattice sites by

$$\mathcal{I} := \{x \in \mathcal{L} \setminus \mathcal{A} \mid x + a_j \in \mathcal{A} \text{ for some } j \in \{1, \dots, 6\}\},$$

and we denote the remaining lattice sites by $\mathcal{C} := \mathcal{L} \setminus (\mathcal{A} \cup \mathcal{I})$; cf. Figure 2.

A general form for the construction of a/c coupling energies is

$$\mathcal{E}_{ac}(y) = \sum_{x \in \mathcal{A}} V(Dy(x)) + \sum_{x \in \mathcal{I}} V_x^i(Dy(x)) + \sum_{x \in \mathcal{C}} V^c(Dy(x)), \quad (2.3)$$

where $V_x^i, x \in \mathcal{I}$, are the interface site potentials that define the method (the atomistic site potential and the continuum site potential are determined by the atomistic model).

For example, if we choose $V_x^i = V$, then we obtain the original *quasicontinuum method* [8] (the QCE method). It is well understood that the QCE method suffers from the occurrence of ghost forces, which result in large modelling errors [1, 6, 7, 12, 16].

In the following we present a new variant of the geometry reconstruction approach [3, 17] for constructing V^i . We define the interface potential as

$$V_x^i(Dy(x)) := V(\mathcal{R}_x Dy(x)), \quad (2.4)$$

where \mathcal{R}_x is a *geometry reconstruction operator* of the general form

$$\mathcal{R}_x Dy(x) := \left(\mathcal{R}_x D_j y(x)\right)_{j=1}^6, \quad \text{and} \quad \mathcal{R}_x D_j y(x) := \sum_{i=1}^6 C_{x,j,i} D_i y(x). \quad (2.5)$$

Here $(C_{x,j,i})_{j,i=1}^6, x \in \mathcal{I}$, are free parameters of the method that can be determined to improve the accuracy of the coupling scheme.

We use the acronym “GR-AC method” (geometry reconstruction-based atomistic-to-continuum coupling method) to describe methods of the type (2.3) where the interface site potential is of the form (2.4).

We aim to determine parameters $C_{x,j,i}$ such that the coupling energy \mathcal{E}_{ac} satisfies the following conditions, which we label, respectively, *local energy consistency* and *local force consistency*:

$$V_x^i(\mathbf{F}_a) = V(\mathbf{F}_a) \quad \forall \mathbf{F} \in \mathbb{R}^{2 \times 2}, \quad \forall x \in \mathcal{I}, \quad \text{and} \quad (2.6)$$

$$f_{ac}(x; y_F) = 0 \quad \forall \mathbf{F} \in \mathbb{R}^{2 \times 2}, \quad \forall x \in \mathcal{L}, \quad (2.7)$$

where $f_{ac}(x; y)$ is the force acting on the atom at site x , initially defined by

$$f_{ac}(x; y) := -\frac{\partial \mathcal{E}_{ac}(y)}{\partial y(x)} \in \mathbb{R}^2 \quad \text{for } y \in \mathcal{Y}_0;$$

however, we immediately see that f_{ac} involves only a sum over a finite set of lattice sites, and hence the formula can be extended to all maps $y : \mathcal{L} \rightarrow \mathbb{R}^2$. In particular, (2.7) is a well-posed condition. Taken together, we call (2.6) and (2.7) the *patch test*. A hybrid energy \mathcal{E}_{ac} of the form (2.3) is called *patch test consistent* if it satisfies both conditions.

In the remainder of the paper, we will determine choices of the parameters $C_{x,j,i}$ for general a/c interface geometries that give patch test consistent coupling methods. Moreover, we will prove that for all parameter choices we determine, the resulting a/c method is first-order consistent at the interface and second-order consistent in the interior of the continuum region. This extends the optimal 1D result in [10].

Remark 2.1. 1. To obtain a method with improved complexity one should use a coarser finite element discretisation in the continuum region. It was seen in [12, 9] that the coarsening step can be understood using standard finite element methodology, and hence we focus only on the modification of the model, and the resulting *modelling errors*.

2. Realistic interaction potentials have singularities for colliding nuclei, i.e., for deformations that are not injective. Clearly, our assumption that $V \in C^3(\mathbb{R}^{2 \times 6})$ contradicts this. It is conceptually easy to admit more general site potentials in our work, however, this would introduce additional technical steps that are of little relevance to the problems we wish to study. \square

2.4. Additional assumptions and notation. We use $|\cdot|$ to denote the ℓ^2 -norm on \mathbb{R}^n , and the Frobenius norm on $\mathbb{R}^{n \times m}$. Generic constants that are independent of the potential (and the constants defined in the following paragraphs) and the underlying deformations are denoted by c . Although it is possible in principle to trace all constants in our proofs, it would require additional non-trivial computations to optimize them.

2.4.1. *Properties of V .* We define notation for partial derivatives of V , for $\mathbf{g} \in \mathbb{R}^{2 \times 6}$, as follows:

$$\partial_j V(\mathbf{g}) := \frac{\partial V(\mathbf{g})}{\partial g_j} \in \mathbb{R}^2, \quad \text{and} \quad \partial_{i,j} V(\mathbf{g}) := \frac{\partial^2 V(\mathbf{g})}{\partial g_i \partial g_j} \in \mathbb{R}^{2 \times 2}, \quad \text{for } i, j \in \{1, \dots, 6\},$$

and similarly, the third derivative $\partial_{i,j,k} V(\mathbf{g}) \in \mathbb{R}^{2 \times 2 \times 2}$, which we will never use explicitly. We will frequently also use the short-hand notation

$$V_{x,j} := \partial_j V(Dy(x)), \quad V_{T,j} := \partial_j V((\partial_T y)\mathbf{a}), \quad \text{and} \quad V_{F,j} := \partial_j V(\mathbf{F}_a),$$

as well as analogous notation for second derivatives and for the site potentials V^c , V^i , and for V^{ac} , which is defined in (3.4).

Interpreting the second and third partial derivatives as multi-linear forms we define the global bounds

$$M_2 := \sum_{i,j=1}^6 \sup_{\mathbf{g} \in \mathbb{R}^{2 \times 6}} \sup_{\substack{h_1, h_2 \in \mathbb{R}^2 \\ |h_1|=|h_2|=1}} \partial_{i,j} V(\mathbf{g})[h_1, h_2], \quad \text{and}$$

$$M_3 := \sum_{i,j,k=1}^6 \sup_{\mathbf{g} \in \mathbb{R}^{2 \times 6}} \sup_{\substack{h_1, h_2, h_3 \in \mathbb{R}^2 \\ |h_1|=|h_2|=|h_3|=1}} \partial_{i,j,k} V(\mathbf{g})[h_1, h_2, h_3].$$

With this notation it is straightforward to show that

$$\sum_{i=1}^6 |\partial_i V(\mathbf{g}) - \partial_i V(\mathbf{h})| \leq M_2 \max_{j=1, \dots, 6} |g_j - h_j|, \quad \text{for } \mathbf{g}, \mathbf{h} \in \mathbb{R}^{2 \times 6}. \quad (2.8)$$

We also assume that V satisfies the point symmetry

$$V((-g_{j+3})_{j=1}^6) = V(\mathbf{g}) \quad \forall \mathbf{g} \in \mathbb{R}^{2 \times 6}. \quad (2.9)$$

The following identities are immediate consequences of this condition:

$$\partial_i V(\mathbf{F}\mathbf{a}) = -\partial_{i+3} V(\mathbf{F}\mathbf{a}), \quad \text{for } i = 1, \dots, 6, \quad \mathbf{F} \in \mathbb{R}^{2 \times 2} \quad (2.10)$$

$$\partial_{ij} V(\mathbf{F}\mathbf{a}) = \partial_{i+3, j+3} V(\mathbf{F}\mathbf{a}), \quad \text{for } i, j = 1, \dots, 6, \quad \mathbf{F} \in \mathbb{R}^{2 \times 2}. \quad (2.11)$$

We will prove results on the class \mathcal{V} , of all site potentials that satisfy (2.9),

$$\mathcal{V} := \{V \in C^3(\mathbb{R}^{2 \times 6}) \mid V \text{ satisfies (2.9)}\}.$$

We will frequently use the following shorthand notation for partial derivatives of V , when there is no ambiguity in their meaning:

$$V_{x,j} := \partial_j V(Dy(x)), \quad V_{\mathbf{F},j} := \partial_j V(\mathbf{F}\mathbf{a}), \quad V_{T,j} := V_{\partial_T y, j},$$

and analogous symbols for other potentials that we will introduce throughout the text.

2.4.2. Linear functionals. For $y \in \mathcal{Y}_0$ and $u \in \mathcal{U}_0$ we denote the directional derivative of \mathcal{E}_a by

$$\langle \delta \mathcal{E}_a(y), u \rangle := \lim_{t \rightarrow 0} \frac{\mathcal{E}_a(y + tu) - \mathcal{E}_a(y)}{t}.$$

We call $\delta \mathcal{E}_a(y)$ the *first variation* of \mathcal{E}_a and understand it as an element of \mathcal{U}_0^* . We use analogous notation for other functionals. This paper is largely concerned with establishing bounds on the *modelling error* $\delta \mathcal{E}_a(y) - \delta \mathcal{E}_{ac}(y)$.

To obtain sharp error estimates in $W^{1,p}$ -like norms, one needs to bound modelling errors in negative Sobolev norms, or, in our case, discrete versions thereof. Let $\ell : \mathcal{U}_0 \rightarrow \mathbb{R}$ be a linear functional, and let $\frac{1}{p} + \frac{1}{p'} = 1$, $1 \leq p, p' \leq \infty$, then we define

$$\|\ell\|_{\mathcal{U}^{-1,p}} := \sup_{\substack{u \in \mathcal{U}_0 \\ \|\partial u\|_{L^{p'}}=1}} \langle \ell, u \rangle.$$

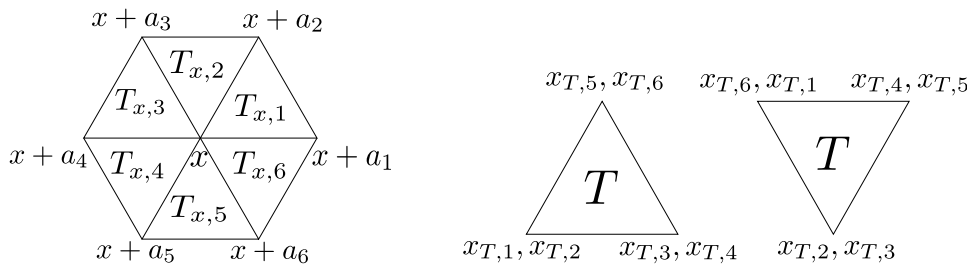


FIGURE 3. Convention for the symbols $T_{x,j}$ and $x_{T,j}$.

2.4.3. *Notation for the lattice and the triangulation.* \mathcal{L} is the set of vertices of \mathcal{T} , and we denote the set of edges of \mathcal{T} by \mathcal{F} , with edge midpoints m_f , $f \in \mathcal{F}$.

For each vertex $x \in \mathcal{L}$ and direction a_j , let $T_{x,j} := \text{conv}\{x, x+a_j, x+a_{j+1}\} \in \mathcal{T}$, $j = 1, \dots, 6$ (see Figure 3). The edge $(x, x+a_j)$ is the intersection of the two elements $T_{x,j}$ and $T_{x,j-1}$. Moreover, let $x_{T,j} \in \mathcal{L}$ be the unique lattice point so that both $x_{T,j}, x_{T,j} + a_j \in T$ (again, see Figure 3).

2.4.4. *Discrete regularity.* To measure regularity or “smoothness” of discrete deformations $y \in \mathcal{B}_0$, we first define the symbols

$$|D^2y(x)| := \max_{i,j=1,\dots,6} |D_i D_j y(x)|, \quad \text{and} \quad |D^3y(x)| := \max_{i,j,k=1,\dots,6} |D_i D_j D_k y(x)|, \quad \text{for } x \in \mathcal{L}.$$

With mild abuse of notation, we then define the norms

$$\|D^2y\|_{\ell^p(\mathcal{A})} := \| |D^2y| \|_{\ell^p(\mathcal{A})}, \quad \text{and} \quad \|D^3y\|_{\ell^p(\mathcal{A})} := \| |D^3y| \|_{\ell^p(\mathcal{A})},$$

for any $\mathcal{A} \subset \mathcal{L}$ and $y \in \mathcal{B}_0$. If the label \mathcal{A} is omitted, then it is assumed that $\mathcal{A} = \mathcal{L}$.

3. CONSTRUCTION OF THE GR-AC METHOD

In this section we carry out an explicit construction of the GR-AC method. Our results are variants of results in [3], however, since our ansatz is different from the one used in [3], and since we wish to be precise about the equivalence of certain conditions, we provide details for all our proofs.

We assume throughout the remainder of the paper that the reconstructed difference $\mathcal{R}_x D_j y(x)$ may depend only on the original differences $D_{j-1}y(x)$, $D_j y(x)$, and $D_{j+1}y(x)$, that is,

$$C_{x,j,i} = 0 \quad \text{for } |(i-j) \bmod 6| > 1, \quad i, j \in \{1, \dots, 6\}, \quad x \in \mathcal{I}. \quad (3.1)$$

For future reference, we call (3.1) the *one-sidedness condition*.

In §3.1 and §3.2 we derive general conditions on the parameters that are independent of the choice of the atomistic region. In §3.3 and §3.4 we then compute explicit sets of parameters.

3.1. Conditions for local energy consistency. We first derive conditions for the local energy consistency condition (2.6).

Proposition 3.1. *Suppose that the parameters $C_{x,j,i}$ satisfy the one-sidedness condition (3.1), then the interface potential V_x^1 satisfies the local energy consistency condition (2.6) for all potentials $V \in \mathcal{V}$ if and only if*

$$C_{x,j,j-1} = C_{x,j,j+1} = 1 - C_{x,j,j}, \quad \text{for } j = 1, \dots, 6. \quad (3.2)$$

Proof. We require that $V_x^i(\mathbf{F}a) = V(\mathbf{F}a)$, for arbitrary $V \in \mathcal{V}$, which is equivalent to

$$\mathbf{F}a_j = \sum_{i=1}^6 C_{x,j,i} \mathbf{F}a_i \quad \text{for } j = 1, \dots, 6.$$

Since this has to hold for arbitrary $\mathbf{F} \in \mathbb{R}^{2 \times 2}$, and in view of (3.1), we obtain the condition

$$a_j = C_{x,j,j-1} a_{j-1} + C_{x,j,j} a_j + C_{x,j,j+1} a_{j+1}$$

Since $a_j = a_{j-1} + a_{j+1}$, this is equivalent to

$$(C_{x,j,j-1} + C_{x,j,j} - 1)a_{j-1} + (C_{x,j,j+1} + C_{x,j,j} - 1)a_{j+1} = 0,$$

and since a_{j-1}, a_{j+1} are linearly independent, we obtain the condition that

$$C_{x,j,j-1} + C_{x,j,j} = 1, \quad \text{and} \quad C_{x,j,j+1} + C_{x,j,j} = 1.$$

Subtracting these two conditions gives $C_{x,j,j+1} = C_{x,j,j-1}$, and hence we obtain (3.2). \square

As a consequence of Assumption (3.1), and Proposition 3.1, we have reduced the number of free parameters to six for each site $x \in \mathcal{I}$. To simplify the subsequent notation, whenever the parameters $C_{x,j,i}$ are chosen to satisfy (3.2), we will write

$$C_{x,j} := C_{x,j,j}, \quad \text{and note that } C_{x,j,j-1} = C_{x,j,j+1} = 1 - C_{x,j}. \quad (3.3)$$

Since it is equivalent to (2.6) we call (3.3) the local energy consistency condition as well.

3.2. Conditions for local force consistency. We rewrite \mathcal{E}_{ac} in terms of a hybrid site potential

$$\mathcal{E}_{\text{ac}}(y) = \sum_{x \in \mathcal{L}} V_x^{\text{ac}}(Dy(x)), \quad \text{where } V_x^{\text{ac}}(\mathbf{g}) := \begin{cases} V^c(\mathbf{g}), & x \in \mathcal{C}, \\ V_x^i(\mathbf{g}), & x \in \mathcal{I}, \\ V(\mathbf{g}), & x \in \mathcal{A}. \end{cases} \quad (3.4)$$

Lemma 3.2. *Suppose that the parameters $(C_{x,j,i})_{i,j=1}^6, x \in \mathcal{I}$, satisfy the one-sidedness condition (3.1) and local energy consistency (3.3). Moreover, let*

$$C_{x,j} := 1 \quad \text{for } x \in \mathcal{A} \quad \text{and} \quad C_{x,j} := 2/3 \quad \text{for } x \in \mathcal{C}, \quad j = 1, \dots, 6, \quad (3.5)$$

and let $(C_{x,j,i})_{i,j=1}^6, x \in \mathcal{A} \cup \mathcal{C}$, be defined to be compatible with (3.1) and (3.3); then

$$-f^{\text{ac}}(x; \text{Fid}) = \sum_{j=1}^6 \sum_{i=1}^6 (C_{x-a_i,j,i} - C_{x,j,i}) V_{\mathbf{F},j} \quad \forall x \in \mathcal{L}. \quad (3.6)$$

Proof. Using the notation (3.4), we have

$$\langle \delta \mathcal{E}_{\text{ac}}(\text{Fid}), u \rangle = \sum_{x \in \mathcal{L}} \sum_{i=1}^6 \partial_i V_x^{\text{ac}}(\mathbf{F}a) \cdot D_i u(x),$$

which immediately gives

$$-f^{\text{ac}}(x; \text{Fid}) = \sum_{i=1}^6 [\partial_i V_{x-a_i}^{\text{ac}}(\mathbf{F}a) - \partial_i V_x^{\text{ac}}(\mathbf{F}a)]. \quad (3.7)$$

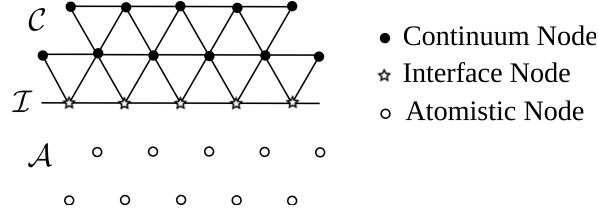


FIGURE 4. The flat interface case.

With the notation introduced in (3.5), we obtain

$$\sum_{i=1}^6 \partial_i V_x^{\text{ac}}(\mathbf{F}\mathbf{a}) \cdot D_i u(x) = \sum_{j=1}^6 V_{\mathbf{F},j} \sum_{i=1}^6 C_{x,j,i} D_i u(x),$$

which implies

$$\partial_i V_x^{\text{ac}}(\mathbf{F}\mathbf{a}) = \sum_{j=1}^6 C_{x,j,i} V_{\mathbf{F},j}. \quad (3.8)$$

Combining (3.8) with (3.7) yields (3.6). \square

Testing (3.6) for all $V \in \mathcal{V}$ and $\mathbf{F} \in \mathbb{R}^{2 \times 2}$, we obtain the next result.

Lemma 3.3. *Suppose that the parameters $(C_{x,j,i})_{i,j=1}^6, x \in \mathcal{I}$, satisfy one-sidedness (3.1) and local energy consistency (3.2). Then \mathcal{E}_{ac} satisfies local force consistency (2.7) for all $V \in \mathcal{V}$ if and only if*

$$\sum_{i=1}^6 (C_{x-a_i,j,i} - C_{x-a_i,j+3,i} - C_{x,j,i} + C_{x,j+3,i}) = 0 \quad \forall j = 1, 2, 3, \quad \forall x \in \mathcal{L}. \quad (3.9)$$

Proof. Using (3.6) and point symmetry (2.10) one readily checks that (3.9) is sufficient for force consistency (2.7). To show that (3.9) is also necessary we test (3.6) with

$$V(\mathbf{g}) = \frac{1}{2} (|g_1 - a_1|^2 + |g_4 - a_4|^2),$$

which clearly belongs to the class \mathcal{V} , to obtain

$$\begin{aligned} -f^{\text{ac}}(x; \text{Fid}) &= \sum_{j=1,4} \sum_{i=1}^6 (C_{x-a_i,j,i} - C_{x,j,i}) (\mathbf{F} - \mathbf{I}) a_j \\ &= \sum_{i=1}^6 (C_{x-a_i,1,i} - C_{x-a_i,4,i} - C_{x,1,i} + C_{x,4,i}) (\mathbf{F} - \mathbf{I}) a_1. \end{aligned}$$

For this expression to vanish for all $\mathbf{F} \in \mathbb{R}^{2 \times 2}$ we obtain precisely (3.9) for $j = 1$. For $j = 2, 3$ the same argument applies. \square

3.3. Explicit parameters for flat interfaces. We now give a characterisation, for a flat a/c interface, of all parameters satisfying the one-sidedness assumption (3.1), which give a patch test consistent a/c method.

Proposition 3.4. *Suppose that $\mathcal{A} = \{x \in \mathcal{L} \mid x_2 < 0\}$, $\mathcal{I} = \{x \in \mathcal{L} \mid x_2 = 0\}$ and $\mathcal{C} = \{x \in \mathcal{L} \mid x_2 > 0\}$ (see Figure 4). Then the parameters $(C_{x,j,i})_{i,j=1}^6$, $x \in \mathcal{I}$, satisfy the one-sidedness condition (3.1), energy consistency (3.3), and force consistency (3.9), if and only if*

$$C_{x,1} = C_{x+a_1,4} \quad \forall x \in \mathcal{I}, \quad \text{and} \quad (3.10)$$

$$C_{x,j} = C_{x+a_1,j} \quad \forall x \in \mathcal{I}, \quad j \in \{2, 3, 5, 6\}, \quad (3.11)$$

where we have used the reduced parameters defined in (3.3).

Proof. One-sidedness (3.1) and energy consistency (3.3) yields the reduced parameters $(C_{x,j})_{j=1}^6$, $x \in \mathcal{I}$, satisfying (3.3). Recall also the extension (3.5) of these parameters for $x \in \mathcal{A} \cup \mathcal{C}$.

Let $\mathcal{I}_+ := \{x + a_2 \mid x \in \mathcal{I}\}$ and $\mathcal{I}_- := \{x - a_2 \mid x \in \mathcal{I}\}$. Clearly, we need to test (3.9) only for $x \in \mathcal{I} \cup \mathcal{I}_- \cup \mathcal{I}_+$. Exploiting the symmetries of the problem it is also clear that we only need to consider $j = 1, 2$.

It is straightforward to verify through direct calculations that any set of coefficients satisfying (3.10), (3.11) satisfies the equivalent force consistency condition (3.9).

Let $j = 1$ and $x \in \mathcal{I}$ then we obtain that (3.10) is necessary from the force consistency condition (3.9), applied at $x + a_2$ or $x + a_6$. Let $j = 2$, then we obtain $C_{x,2} = C_{x+a_1,2}$ from the force consistency condition (3.9) applied at $x + a_2$. Therefore, (3.10) and (3.11) are also necessary. \square

Remark 3.1. We observe that the coefficients $(C_{x,i,j})_{i,j=1}^6$, $x \in \mathcal{I}$, are not unique, but that we have considerable freedom in the construction of the GR-AC method: For each direction a_i that is not aligned with the interface, there is a free parameter, while for each edge $(x, x + a_1)$ lying on the interface, there is one additional free parameter. This freedom will be reduced in the case of corners. \square

3.4. Explicit parameters for general interfaces. For general interface geometries we make the following separation assumption. This assumption requires that, if the atomistic region can be decomposed into several connected components, then they must be separated by at least four ‘‘lattice hops’’.

Assumption 3.5. *Each vertex $x \in \mathcal{I}$ has exactly two neighbours in \mathcal{I} , and at least one neighbour in \mathcal{C} .*

As in the flat interface case, we can completely characterise all parameters within the one-sidedness assumption, which satisfy the patch test.

Proposition 3.6. *Let $\mathcal{A} \subset \mathcal{L}$ be defined in such a way that the interface set \mathcal{I} satisfies Assumption 3.5, and is not planar. Then the parameters $(C_{x,j,i})_{i,j=1}^6$, $x \in \mathcal{I}$, satisfy the one-sidedness condition (3.1), energy consistency (3.3), and force consistency (3.9), if and only*

if

$$C_{x,j} = C_{x+a_j,j+3} \quad \forall x \in \mathcal{I}, \quad x + a_j \in \mathcal{I}, \quad (3.12)$$

$$C_{x,j} = 1 \quad \forall x \in \mathcal{I}, \quad x + a_j \in \mathcal{A}, \quad \text{and} \quad (3.13)$$

$$C_{x,j} = 2/3 \quad \forall x \in \mathcal{I}, \quad x + a_j \in \mathcal{C}, \quad (3.14)$$

where $(C_{x,j})_{j=1}^6$, $x \in \mathcal{I}$, are the reduced parameters defined in (3.3).

Proof. As in the flat interface case, one-sidedness (3.1) and energy consistency (3.3) are equivalent to having the reduced parameters $(C_{x,j})_{j=1}^6$, $x \in \mathcal{I}$, satisfying (3.3). Recall also the extension (3.5) of these parameters for $x \in \mathcal{A} \cup \mathcal{C}$.

Let $\mathcal{I}_+ := \{x \in \mathcal{C} \mid \exists a_j, x + a_j \in \mathcal{I}\}$ and $\mathcal{I}_- := \{x \in \mathcal{A} \mid \exists a_j, x + a_j \in \mathcal{I}\}$. We need to test (3.9) only for $x \in \mathcal{I} \cup \mathcal{I}_- \cup \mathcal{I}_+$. The necessity of (3.12) follows as in the flat interface case. The necessity of (3.13) and (3.14) can be obtained by testing the corner sites in \mathcal{I}_\pm in the interface geometry depicted in Figure 2.

To see that (3.12)–(3.14) are also sufficient one notes, first, that the corresponding coefficients always provide zero contribution on each edge for the sum in (3.9). Computing the force at $x \in \mathcal{I}_+$ we see that the contribution from V^i is the same as from V^c , and must therefore cancel, since the pure Cauchy–Born model passes (3.9). For $x \in \mathcal{I}_-$ the same argument applies.

It remains to test (3.9) for $x \in \mathcal{I}$, at corners. Since (3.9) is a local condition, and due to Assumption 3.5, one may assume that the interface has only one corner. Since all other sites are in equilibrium, and since the forces are conservative, it follows that the corner must also be in equilibrium.

(Alternatively, one may check (3.9) through explicit computations for the corner geometry shown in Figure 2. All other geometries can be reduced to this one by symmetry.) \square

Remark 3.2. We observe that, for a general interface, we only have freedom to choose the geometric reconstruction parameters along the interface, namely, for each interface edge there is one free parameter. \square

4. CONSISTENCY OF THE CAUCHY–BORN APPROXIMATION

Before we embark on the analysis of the GR-AC method (2.3), we establish a sharp consistency estimate for Cauchy–Born approximation. Related results were established in [4], which require more stringent conditions on the smoothness of the deformation field. For the analysis of a/c methods a sharp consistency estimate, such as Theorem 4.2, is useful. In the remainder of the section we establish technical results that are useful for the subsequent consistency analysis of the GR-AC method.

4.1. Second-order consistency. A natural way to represent the first variation of \mathcal{E}_a is

$$\langle \delta \mathcal{E}_a(y), u \rangle = \sum_{x \in \mathcal{L}} \sum_{j=1}^6 \partial_j V(Dy(x)) \cdot D_j u(x) = \sum_{x \in \mathcal{L}} \sum_{j=1}^6 V_{x,j} \cdot D_j u(x), \quad (4.1)$$

where we use the notation $V_{x,j} := \partial_j V(Dy(x))$. This representation can be interpreted as a sum over mesh edges. By contrast, the most natural representation of $\delta \mathcal{E}_c$ is

$$\langle \delta \mathcal{E}_c(y), u \rangle = \sum_{T \in \mathcal{T}} |T| \partial W(\partial_T y) : \partial_T u. \quad (4.2)$$

To estimate $\delta\mathcal{E}_a - \delta\mathcal{E}_c$ we will rewrite (4.2) in a form mimicking (4.1). The opposite approach is also possible, but does not lead as easily to second-order consistency estimates.

Lemma 4.1. *For $y \in \mathcal{Y}_0, T \in \mathcal{T}$, let $V_{T,j} := \partial_j V(\partial_T y \cdot \mathbf{a})$; then*

$$\langle \delta\mathcal{E}_c(y), u \rangle = \sum_{x \in \mathcal{L}} \sum_{j=1}^3 (V_{T_{x,j},j} + V_{T_{x,j-1},j}) \cdot D_j u(x), \quad \forall u \in \mathcal{U}_0, \quad \text{and} \quad (4.3)$$

$$\langle \delta\mathcal{E}_a(y), u \rangle = \sum_{x \in \mathcal{L}} \sum_{j=1}^3 (V_{x,j} - V_{x+a_j,j+3}) \cdot D_j u(x), \quad \forall u \in \mathcal{U}_0. \quad (4.4)$$

Proof. It is easy to see that

$$\partial W(\mathbf{F}) = \frac{1}{\Omega_0} \sum_{j=1}^6 \partial_j V(\mathbf{F}\mathbf{a}) \otimes a_j, \quad (4.5)$$

and hence, using $\Omega_0 = 2|T|$ and $\partial_T u \cdot a_j = D_j u(x_{T,j})$,

$$\langle \delta\mathcal{E}_c(y), u \rangle = \frac{1}{\Omega_0} \sum_{T \in \mathcal{T}} |T| \sum_{j=1}^6 [V_{T,j} \otimes a_j] : \partial_T u = \frac{1}{2} \sum_{T \in \mathcal{T}} \sum_{j=1}^6 V_{T,j} \cdot D_j u(x_{T,j}).$$

Every edge appears twice in this sum since it is shared between two elements; hence we obtain the edge representation

$$\langle \delta\mathcal{E}_c(y), u \rangle = \sum_{x \in \mathcal{L}} \sum_{j=1}^6 \frac{1}{2} (V_{T_{x,j},j} + V_{T_{x,j-1},j}) \cdot D_j u(x) \quad \forall u \in \mathcal{U}_0. \quad (4.6)$$

Since $D_{j+3}u(x+a_j) = -D_ju(x)$, and using $V_{T,j+3} = -V_{T,j}$ (see (2.10)) we can reduce this sum as follows:

$$\begin{aligned} \langle \delta\mathcal{E}_c(y), u \rangle &= \sum_{x \in \mathcal{L}} \sum_{j=1}^3 \frac{1}{2} (V_{T_{x,j},j} + V_{T_{x,j-1},j} - V_{T_{x,j},j+3} - V_{T_{x,j-1},j+3}) \cdot D_j u(x) \\ &= \sum_{x \in \mathcal{L}} \sum_{j=1}^3 (V_{T_{x,j},j} + V_{T_{x,j-1},j}) \cdot D_j u(x). \end{aligned}$$

This concludes the proof of (4.3).

For the proof of (4.4) one only needs to use the identity $D_{j+3}u(x+a_j) = -D_ju(x)$. \square

Theorem 4.2. *Let $y \in \mathcal{Y}_0$, then*

$$\|\delta\mathcal{E}_a(y) - \delta\mathcal{E}_c(y)\|_{\mathcal{Q}_{-1,p}} \leq c(M_2 \|D^3 y\|_{\ell^p} + M_3 \|D^2 y\|_{\ell^{2p}}^2) \quad (4.7)$$

where M_2, M_3 are defined in §2.4.1.

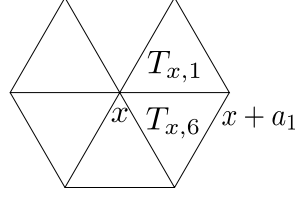


FIGURE 5. Visualisation of the proof of Theorem 4.2.

Proof. It is useful to visualize this proof using Figure 5, and Figure 3 for additional detail. From Lemma 4.1 we obtain

$$\langle \delta \mathcal{E}_a(y) - \delta \mathcal{E}_c(y), u \rangle = \sum_{x \in \mathcal{L}} \sum_{j=1}^3 \delta_j(x) \cdot D_j u(x), \quad (4.8)$$

$$\text{where} \quad \delta_j(x) := V_{x,j} - V_{x+a_j,j+3} - V_{T_{x,j},j} - V_{T_{x,j-1},j}. \quad (4.9)$$

In the following we estimate $\delta_1(x)$ only; the remaining estimates follow by symmetry.

Let $F_+ := \partial_{T_{x,1}} y$ and $F_- := \partial_{T_{x,6}} y$, then $V_{T_{x,1},1} = V_{F_+,1}$ and $V_{T_{x,6},1} = V_{F_-,1}$. Moreover we can Taylor expand

$$\begin{aligned} V_{x,1} &= V_{F_+,1} + \sum_{i=1}^6 V_{F_+,1i}(D_i y(x) - F_+ a_i) + O(|D^2 y(x)|^2), \quad \text{and similarly} \\ -V_{x+a_1,4} &= -V_{F_-,4} - \sum_{j=1}^6 V_{F_-,4j}(D_j y(x+a_1) - F_- a_j) + O(|D^2 y(x)|^2) \\ &= V_{F_-,1} - \sum_{j=1}^6 V_{F_-,1(i+3)}(D_i y(x+a_1) - F_- a_i) + O(|D^2 y(x)|^2) \\ &= V_{F_-,1} + \sum_{j=1}^6 V_{F_-,1i}(-D_{i+3} y(x+a_1) - F_- a_i) + O(|D^2 y(x)|^2). \end{aligned}$$

A careful analysis of the remainder shows that $O(|D^2 y(x)|^2) \leq \frac{1}{2} \sum_{i,j=1}^6 |\partial_{1ij} V(\boldsymbol{\theta})| |D^2 y(x)|^2$ for some $\boldsymbol{\theta} \in \mathbb{R}^{2 \times 6}$. In the remainder of the proof we will suppress the argument $\boldsymbol{\theta}$.

Clearly, $V_{F_-,1i} - V_{F_+,1i} = O(|D^2 y(x)|) \leq \sum_{j=1}^6 |\partial_{1ij} V| |D^2 y(x)|$, and hence we can deduce that

$$\begin{aligned} \delta_1(x) &= \sum_{i=1}^6 V_{F_+,1i}(D_i y(x) - F_+ a_i - D_{i+3} y(x+a_1) - F_- a_i) + O(|D^2 y(x)|^2) \\ &= \sum_{i=1}^6 V_{F_+,1i}(D_i y(x) - D_i y(x_i^+) + D_i y(x+a_1 - a_i) - D_i y(x_i^-)) + O(|D^2 y(x)|^2) \\ &=: \sum_{i=1}^6 V_{F_+,1i} \varepsilon_i + O(|D^2 y(x)|^2), \end{aligned}$$

where $x_i^+ := x_{T_{x,1,i}}$ and $x_i^- := x_{T_{x,6,i}}$. (These are simply the vertices in the two adjacent elements such that the identities $F_{\pm a_i} = D_i y(x_i^{\pm})$ hold.)

Tracing the previous Taylor expansions, we see that, in the last estimate, $O(|D^2 y(x)|^2) \leq 2 \sum_{i,j=1}^6 |\partial_{1ij} V| |D^2 y(x)|^2$.

We compute ε_3 in detail but only give the results for the remaining coefficients:

$$\begin{aligned} \varepsilon_3 &= D_3 y(x) - D_3 y(x + a_1) + D_3 y(x + a_1 - a_3) - D_3 y(x - a_3) \\ &= -D_1 D_3 y(x) + D_1 D_3 y(x - a_3) = D_6 D_1 D_3 y(x). \end{aligned}$$

By performing similar calculations for $i = 1, 2, 4, 5, 6$, one finds

$$\varepsilon_1 = \varepsilon_2 = \varepsilon_6 = 0, \quad \varepsilon_4 = D_1 D_1 D_4 y(x), \quad \text{and} \quad \varepsilon_5 = D_1 D_2 D_5 y(x);$$

hence we obtain that $\delta_j(x) = O(|D^2 y(x)|^2 + |D^3 y(x)|)$ (recall that we assumed, without loss of generality, that $j = 1$), where $O(|D^3 y(x)|) \leq \sum_{i=3,4,5} |\partial_{1,i} V| |D^3 y(x)|$.

Combining these estimates, we obtain

$$\langle \delta \mathcal{E}_a(y) - \delta \mathcal{E}_c(y), u \rangle \leq \left(\sum_{x \in \mathcal{L}} \sum_{j=1}^3 |\delta_j(x)|^p \right)^{1/p} \left(\sum_{x \in \mathcal{L}} \sum_{j=1}^3 |D_j u(x)|^{p'} \right)^{1/p'}.$$

Elementary estimates yield

$$\begin{aligned} \left(\sum_{x \in \mathcal{L}} \sum_{j=1}^3 |\delta_j(x)|^p \right)^{1/p} &\leq M_2 \|D^3 y\|_{\ell^p} + M_3 \|D^2 y\|_{\ell^{2p}}^2, \quad \text{and} \\ \left(\sum_{x \in \mathcal{L}} \sum_{j=1}^3 |D_j u(x)|^{p'} \right)^{1/p'} &\leq (2\sqrt{3})^{1/p'} \left(\sum_{T \in \mathcal{T}} |T| |\partial_T u|^{p'} \right)^{1/p'}, \end{aligned}$$

from which the result follows immediately. \square

In the following subsections, we derive technical results related to Theorem 4.2, in preparation for the proof of consistency of the GR-AC method.

4.2. Stress tensors. We can re-interpret Theorem 4.2 in terms of a second-order error estimate for certain stress tensors. If, for some $y \in \mathcal{Y}_0$, there exist tensor fields $\Sigma_a(y; \bullet), \Sigma_c(y; \bullet) \in P_0(\mathcal{T})^{2 \times 2}$, which satisfy the identities

$$\langle \delta \mathcal{E}_a(y), u \rangle = \sum_{T \in \mathcal{T}} |T| \Sigma_a(y; T) : \partial_T u, \quad \text{and} \quad (4.10)$$

$$\langle \delta \mathcal{E}_c(y), u \rangle = \sum_{T \in \mathcal{T}} |T| \Sigma_c(y; T) : \partial_T u \quad (4.11)$$

then we call Σ_a an atomistic stress tensor and Σ_c a continuum stress tensors.

It follows from (4.1) and (4.2) that

$$\Sigma_a(y; T) := \frac{1}{\Omega_0} \sum_{j=1}^6 V_{x_{T,j},j} \otimes a_j, \quad \text{and} \quad (4.12)$$

$$\Sigma_c^1(y; T) := \partial W(\partial_T y) = \frac{1}{\Omega_0} \sum_{j=1}^6 V_{T,j} \otimes a_j \quad (4.13)$$

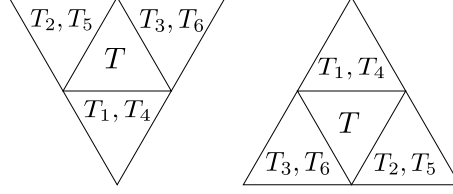


FIGURE 6. Notation for neighbouring triangles of $T \in \mathcal{T}$.

satisfy (4.10) and (4.11), respectively. As we will see immediately, they are not the unique choices.

In the following calculation (and later on as well) we denote by T_j the unique neighbouring element of $T \in \mathcal{T}$, which shares an edge with direction a_j with T ; see Figure 6.

With this notation, and using the fact that $D_j u(x_{T,j}) = D_j u(x_{T_j,j})$, we observe that

$$\begin{aligned}
 \langle \delta \mathcal{E}_c(y), u \rangle &= \sum_{T \in \mathcal{T}} |T| \frac{1}{\Omega_0} \sum_{j=1}^6 V_{T,j} \cdot D_j u(x_{T,j}) \\
 &= \sum_{T \in \mathcal{T}} |T| \frac{1}{\Omega_0} \sum_{j=1}^6 \frac{1}{2} (V_{T,j} + V_{T_j,j}) \cdot D_j u(x_{T,j}) \\
 &= \sum_{T \in \mathcal{T}} |T| \left\{ \frac{1}{\Omega_0} \sum_{j=1}^6 \frac{1}{2} (V_{T,j} + V_{T_j,j}) \otimes a_j \right\} : \partial_T u \quad \forall u \in \mathcal{U}_0,
 \end{aligned} \tag{4.14}$$

which yields the alternative continuum stress tensor

$$\Sigma_c^2(y; T) := \frac{1}{\Omega_0} \sum_{j=1}^6 \frac{1}{2} (V_{T,j} + V_{T_j,j}) \otimes a_j. \tag{4.15}$$

Furthermore, if we write the Cauchy–Born energy in terms of the site energy (2.2), and apply the procedure used to derive Σ_a , then we obtain a third variant of the continuum stress tensor:

$$\Sigma_c^3(y; T) := \frac{1}{\Omega_0} \sum_{j=1}^6 V_{x_{T,j},j}^c \otimes a_j. \tag{4.16}$$

We see that stress tensors are not uniquely defined by (4.11) and (4.10). This causes analytical difficulties when deriving consistency error estimates, which strongly depend on the choice of the stress tensors. For example we will show in the following result that Σ_c^2 is second-order consistent. By contrast, Σ_c^1 and Σ_c^3 are only first-order consistent (cf. Remark 4.1).

Lemma 4.3. *Let $y \in \mathcal{Y}_0$, then*

$$|\Sigma_a(y; T) - \Sigma_c^2(y; T)| \leq c(M_3 |D^2 y(x)|^2 + M_2 |D^3 y(x)|) \tag{4.17}$$

for all $T \in \mathcal{T}, x \in T$.

Proof. This estimate is obtained by reversing the construction of Σ_c^2 in (4.14), and applying the estimates obtained in the proof of Theorem 4.2. \square

Remark 4.1. Taylor expansions show that Σ_c^k , $k = 1, 3$, are only first-order consistent,

$$|\Sigma_a(y; T) - \Sigma_c^k(y; T)| \leq cM_2|D^2y(x)| \quad \text{for } x \in T,$$

but that a second-order estimate such as (4.17) would be false. The first-order estimate can also be obtained from the fact that $\Sigma_a(y_F; \bullet) = \Sigma_c^k(y_F; \bullet) = \partial W(\mathbf{F})$ for all $\mathbf{F} \in \mathbb{R}^{2 \times 2}$. \square

4.3. Divergence-free stress tensors. In the previous subsection, we have seen that the stress functions defined in (4.10) and (4.11) are not unique. It is therefore crucial to characterize all divergence-free tensors, which is the purpose of the present section. We call a piecewise constant tensor $\sigma \in P_0(\mathcal{T})^{2 \times 2}$ *divergence free*, if it satisfies

$$\int_{\mathbb{R}^2} \sigma : \partial u \, dx = \sum_{T \in \mathcal{T}} |T| \sigma(T) : \partial_T u = 0 \quad \forall u \in \mathcal{U}_c. \quad (4.18)$$

Divergence-free tensors can be characterised as 2D-curls of non-conforming Crouzeix–Raviart finite elements. Let $N_1(\mathcal{T})$ be defined by

$$N_1(\mathcal{T}) := \left\{ v : \mathbb{R}^2 \rightarrow \mathbb{R} \mid \begin{array}{l} v|_{\text{int}(T)} \text{ is linear for each } T \in \mathcal{T} \\ v \text{ is continuous at all edge midpoints} \end{array} \right\}.$$

The degrees of freedom for functions $w \in N_1(\mathcal{T})$ are the nodal values at edge midpoints, $w(q_f)$, $f \in \mathcal{F}$, and the associated nodal basis functions are denoted by ζ_f .

We have the following characterization lemma [13] for divergence free tensor fields. Although we will never use the equivalence of the characterisation explicitly, it motivates much of our subsequent analysis. ***!***

Lemma 4.4. *A tensor field $\sigma \in P_0(\mathcal{T})^{2 \times 2}$ is divergence-free (i.e., satisfies (4.18)) if and only if there exists $\psi \in N_1(\mathcal{T})^2$, such that $\sigma = \partial \psi \mathbf{J}$, where \mathbf{J} is the rotation by $\pi/2$.*

Proof. It is easy to show that every tensor of the form $\sigma = \partial w \mathbf{J}$, $w \in N_1(\mathcal{T})^2$ satisfies (4.18), by checking the result for a single nodal basis function $\psi = \zeta_f$.

To show the reverse, let Ω be a simply connected domain, which is a union of triangles $T \in \mathcal{T}$. Suppose that the number of vertices in Ω is $\#V$, the number of interior vertices is $\#V_I$, the number of edges in Ω is $\#E$, and the number of triangles in Ω is $\#T$.

We test (4.18) for all $u \in \mathcal{U}_0$ that are non-zero only in the interior of Ω . The dimension of all $\sigma \in P_0(\Omega)^{2 \times 2}$ satisfying (4.18) for those u can be at most $4\#T - 2\#V_I$. On the other hand, the dimension of $N_1(\Omega)^2$ is $2\#E$ and the dimension of rotated gradients of Crouzeix–Raviart functions, denoted by $\partial N_1(\Omega)^2 \mathbf{J}$, is $2\#E - 2$. We will show below that the following formula holds:

$$4\#T - 2\#V_I \leq 2\#E - 2, \quad (4.19)$$

which immediately implies that the subspace of divergence-free tensor coincides with $\partial N_1(\Omega)^2 \mathbf{J}$. Moreover, the representation is of course unique (up to a shift) and therefore independent of the choice of the domain.

To prove (4.19), we use Euler’s formula,

$$\#V - \#E + \#T = 1, \quad (4.20)$$

and the identify

$$3\#F = 2\#E - \#V + \#V_I, \quad (4.21)$$

which is obtained by a simple counting argument. (Note that $\#V - \#V_I$ is the number of boundary edges.) Subtracting (4.20) from (4.21) yields (4.19). \square

4.4. Continuum stress tensor correctors. We have different forms of continuum stress Σ_c^1 , Σ_c^2 and Σ_c^3 , which all can be used to represent $\delta\mathcal{E}_c$ in the form (4.11), and hence their differences must be divergence free. Lemma 4.4 characterises the form of these differences and motivates the following result.

Lemma 4.5. *Let $y \in \mathcal{Y}_0$, then there exists a corrector $\psi^{23}(y; \bullet) \in N_1(\mathcal{T})^2$ satisfying the following two properties:*

$$\text{Corrector property:} \quad \Sigma_c^3(y; T) - \Sigma_c^2(y; T) = \partial\psi^{23}(y; T)\mathbf{J} \quad \forall T \in \mathcal{T}; \quad (4.22)$$

$$\text{Lipschitz property:} \quad |\psi^{23}(y; m_f)| \leq \frac{1}{6}M_2\|D^2y\|_{\ell^\infty(f \cap \mathcal{L})} \quad \forall f \in \mathcal{F}. \quad (4.23)$$

Proof. Property (4.22) follows of course from Lemma 4.4, however, to establish (4.23) we require an explicit expression of ψ^{23} . We give the details of the proof for the case of an upward pointing triangle $T \in \mathcal{T}$ (cf. the left configuration in Figure 6). An elementary computation, starting from (4.15) and (4.16) and using the symmetry property (2.10), yields

$$\Sigma_c^3(y; T) - \Sigma_c^2(y; T) = \frac{1}{3\Omega_0} [(V_{T,1} - V_{T_{1,1}}) + (V_{T,3} - V_{T_{1,3}}) + (V_{T,5} - V_{T_{1,5}})] \otimes a_1 + \dots,$$

where “...” stands for terms that are symmetric to the ones in the first line. The directions a_1, a_3, a_5 are chosen anti-clockwise with respect to the element T .

We now observe that, if f is an edge of T with direction a_j , $j \in \{1, 3, 5\}$, then

$$\partial\zeta_f\mathbf{J} = \begin{cases} -\frac{2}{\Omega_0}a_j^\top, & \text{in } T, \\ \frac{2}{\Omega_0}a_j^\top, & \text{in } T_j. \end{cases} \quad (4.24)$$

Let f be the edge of T with direction a_1 , then choosing

$$\psi^{23}(y; m_f) := \frac{1}{6}(V_{T,1} - V_{T_{1,1}}) + \frac{1}{6}(V_{T,3} - V_{T_{1,3}}) + \frac{1}{6}(V_{T,5} - V_{T_{1,5}}), \quad (4.25)$$

and making analogous choices for the remaining edges, we obtain (4.22).

With this explicit representation we can now prove the Lipschitz property (4.23). Let f denote the edge of T with direction a_1 , $\mathbf{F} := \partial_T y$ and $\mathbf{F}_1 := \partial_{T_1} y$; then

$$\begin{aligned} |\psi^{23}(y; m_f)| &\leq \frac{1}{6}|V_{\mathbf{F}_1,1} - V_{\mathbf{F},1}| + \frac{1}{6}|V_{\mathbf{F}_1,2} - V_{\mathbf{F},2}| + \frac{1}{6}|V_{\mathbf{F}_1,3} - V_{\mathbf{F},3}| \\ &\leq \frac{1}{6} \sum_{j=1}^6 (|V_{,1j}| + |V_{,2j}| + |V_{,3j}|) |(\mathbf{F}_1 - \mathbf{F})a_j| \leq \frac{1}{6}M_2 \max_{j=1,\dots,6} |(\mathbf{F}_1 - \mathbf{F})a_j|, \end{aligned} \quad (4.26)$$

where $V_{,1j} = \partial_{1j}V(\mathbf{G}_j \cdot \mathbf{a})$ for some $\mathbf{G}_j \in \mathbb{R}^{2 \times 2}$, and M_2 is defined in §2.4.1. One now verifies that

$$(\mathbf{F}_1 - \mathbf{F})a_1 = 0, \quad (\mathbf{F}_1 - \mathbf{F})a_2 = D_6 D_2 y(x_{T,1}), \quad \text{and} \quad (\mathbf{F}_1 - \mathbf{F})a_3 = D_5 D_3 y(x_{T,5}),$$

which implies

$$\max_{j=1,\dots,6} |(\mathbf{F}_1 - \mathbf{F})a_j| \leq \max(|D^2y(x_{T,1})|, |D^2y(x_{T,4})|).$$

Combining this estimate with (4.26) we obtain (4.23) for edges aligned with a_1 . The remaining cases follow from symmetry considerations. \square

5. CONSISTENCY OF THE GR-AC METHOD

We are now ready to state the second main result of this paper. The proof is established in §5.1 through §5.3. For the remainder of this section we assume that the hypotheses stated in Theorem 5.1 hold.

Theorem 5.1. *Let \mathcal{E}_{ac} be defined by (3.4), with parameters $(C_{x,i,j})_{i,j=1}^6$, $x \in \mathcal{I}$, satisfying the one-sidedness condition (3.1), as well as the patch test conditions (2.6) and (2.7). Suppose in addition that the parameters are bounded, that is,*

$$\sup_{x \in \mathcal{I}} \max_{j,i \in \{1, \dots, 6\}} |C_{x,j,i}| =: \bar{C} < +\infty.$$

Then there exists a constant $C_{\mathcal{I}} = C_{\mathcal{I}}(\bar{C})$, such that

$$\|\delta \mathcal{E}_{\text{ac}}(y) - \delta \mathcal{E}_{\text{a}}(y)\|_{\mathcal{W}^{-1,p}} \leq c(C_{\mathcal{I}} M_2 \|D^2 y\|_{\ell^p(\mathcal{I}^{\text{ext}})} + M_2 \|D^3 y\|_{\ell^p(\mathcal{C})} + M_3 \|D^2 y\|_{\ell^{2p}(\mathcal{C})}^2), \quad (5.1)$$

where $\mathcal{I}^{\text{ext}} := \{x \in \mathcal{L} \mid \text{dist}(x, \mathcal{I}) \leq 1\}$ is an extended interface region.

5.1. An a/c stress tensor. Following the construction of Σ_{a} in (4.12) (with \mathcal{E}_{a} replaced by \mathcal{E}_{ac}), we obtain a representation of $\delta \mathcal{E}_{\text{ac}}$ in terms of an a/c stress Σ_{ac} : let $y \in \mathcal{Y}_0$ and $u \in \mathcal{U}_0$, then

$$\langle \delta \mathcal{E}_{\text{ac}}(y), u \rangle = \sum_{T \in \mathcal{T}} |T| \Sigma_{\text{ac}}(y; T) : \partial_T u, \quad \text{where} \quad (5.2)$$

$$\Sigma_{\text{ac}}(y; T) := \frac{1}{\Omega_0} \sum_{j=1}^6 V_{x_{T,j},j}^{\text{ac}} \otimes a_j, \quad (5.3)$$

and we recall that $V_{x,j}^{\text{ac}} = \partial_j V^{\text{ac}}(x; Dy(x))$. We now require the following additional notation:

$$\begin{aligned} \mathcal{T}_{\mathcal{A}} &:= \{T \in \mathcal{T} \mid T \cap (\mathcal{I} \cup \mathcal{C}) = \emptyset\}, & \mathcal{F}_{\mathcal{A}} &:= \mathcal{F} \cap \mathcal{T}_{\mathcal{A}}, \\ \mathcal{T}_{\mathcal{C}} &:= \{T \in \mathcal{T} \mid T \cap (\mathcal{I} \cup \mathcal{A}) = \emptyset\}, & \mathcal{F}_{\mathcal{C}} &:= \mathcal{F} \cap \mathcal{T}_{\mathcal{C}}, \\ \mathcal{T}_{\mathcal{I}} &:= \mathcal{T} \setminus (\mathcal{T}_{\mathcal{C}} \cup \mathcal{T}_{\mathcal{A}}), \quad \text{and} & \mathcal{F}_{\mathcal{I}} &:= \mathcal{F} \setminus (\mathcal{F}_{\mathcal{C}} \cup \mathcal{F}_{\mathcal{A}}). \end{aligned} \quad (5.4)$$

Lemma 5.2. (i) *Let Σ_{ac} be defined by (5.3), then, for all $y \in \mathcal{Y}_0$,*

$$\Sigma_{\text{ac}}(y; T) = \Sigma_{\text{a}}(y; T) \quad \forall T \in \mathcal{T}_{\mathcal{A}}, \quad \text{and} \quad (5.5)$$

$$\Sigma_{\text{ac}}(y; T) = \Sigma_{\mathcal{C}}^3(y; T) \quad \forall T \in \mathcal{T}_{\mathcal{C}}. \quad (5.6)$$

(ii) *Let $\mathbf{F} \in \mathbb{R}^{2 \times 2}$; then there exists a unique $\psi^{\text{ac}}(\mathbf{F}; \bullet) \in \mathbf{N}_1(\mathcal{T})^2$ such that*

$$\Sigma_{\text{ac}}(y_{\mathbf{F}}; T) - \Sigma_{\text{a}}(y_{\mathbf{F}}; T) = \partial \psi^{\text{ac}}(\mathbf{F}; T) \mathbf{J} \quad \forall T \in \mathcal{T}, \quad \text{and} \quad (5.7)$$

$$\psi^{\text{ac}}(\mathbf{F}; m_f) = 0 \quad \forall f \in \mathcal{F}_{\mathcal{A}} \cup \mathcal{F}_{\mathcal{C}}. \quad (5.8)$$

Moreover, there exists L_{ac} depending only on \bar{C} such that the following Lipschitz property holds:

$$|\psi^{\text{ac}}(\mathbf{F}; m_f) - \psi^{\text{ac}}(\mathbf{G}; m_f)| \leq L_{\text{ac}} M_2 |\mathbf{F} - \mathbf{G}| \quad \forall \mathbf{F}, \mathbf{G} \in \mathbb{R}^{2 \times 2}, \quad f \in \mathcal{F}_{\mathcal{I}}. \quad (5.9)$$

Proof. (i) Properties (5.5) and (5.6) follow immediately from the definitions of the three tensors and the sets \mathcal{T}_A and \mathcal{T}_C , and are independent of the choice of the reconstruction parameters at the interface.

(ii) Since \mathcal{E}_{ac} is assumed to satisfy local force consistency (2.7), we have

$$0 = \langle \delta \mathcal{E}_{ac}(y_F) - \delta \mathcal{E}_a(y_F), u \rangle = \sum_{T \in \mathcal{T}} |T| (\Sigma_{ac}(y_F; T) - \Sigma_a(y_F; T)) : \partial_T u \quad \forall u \in \mathcal{U}_0,$$

and hence $\Sigma_{ac}(y_F; \bullet) - \Sigma_a(y_F; \bullet)$ is divergence free. According to Lemma 4.4 there exists a function $\psi^{ac} \in N_1(\mathcal{T})^2$, which is unique up to a constant shift, such that (5.7) holds. Property (5.8) uniquely determines the shift.

As a matter of fact, it is highly non-trivial whether (5.8) can be satisfied, and it is in principle possible that the corrections “propagate” into the continuum region [9]. We postpone the detailed computations required to prove this to Appendix 6.1 and 6.2, where we then also give a proof of the Lipschitz property (5.9). \square

5.2. The modified a/c stress. The function $\psi^{ac}(\mathbf{F}; \bullet)$ obtained in Lemma 5.3 provides the divergence-free corrector for $\Sigma_{ac} - \Sigma_a$ for homogeneous deformations. We now construct the corrector for nonlinear deformations: First, for each $f \in \mathcal{T}_I$, $f = T_+ \cap T_-$, we set

$$\mathbf{F}_f(y) := \frac{1}{2} (\partial_{T_+} y + \partial_{T_-} y).$$

We can now define the corrector function for $y \in \mathcal{Y}_0$ as

$$\hat{\psi}^{ac}(y; \bullet) := \sum_{f \in \mathcal{T}_I} \psi^{ac}(\mathbf{F}_f(y); m_f) \zeta_f + \sum_{f \in \mathcal{T}_C} \psi^{23}(y; m_f) \zeta_f, \quad (5.10)$$

and the corresponding modified stress function

$$\hat{\Sigma}_{ac}(y; T) := \Sigma_{ac}(y; T) - \partial \hat{\psi}^{ac}(y; T) \mathbf{J}, \quad \text{for } T \in \mathcal{T}. \quad (5.11)$$

We show in Remark 6.1, that $\hat{\psi}^{ac}$ is non-trivial, that is, there exists no choice of parameters for which $\hat{\psi}^{ac} = 0$, even under purely homogeneous deformations.

The properties of the modified stress function $\hat{\Sigma}_{ac}$ are summarized in the following lemma.

Lemma 5.3. *Let $\hat{\Sigma}_{ac}$ be defined by (5.11), and $y \in \mathcal{Y}_0$; then the following identities hold:*

$$\langle \delta \mathcal{E}_{ac}(y), u \rangle = \sum_{T \in \mathcal{T}} |T| \hat{\Sigma}_{ac}(y; T) : \partial_T u \quad \forall u \in \mathcal{U}_0; \quad (5.12)$$

$$\hat{\Sigma}_{ac}(y; T) = \Sigma_a(y; T) \quad \forall T \in \mathcal{T}_A; \quad (5.13)$$

$$\hat{\Sigma}_{ac}(y; T) = \Sigma_c^2(y; T) \quad \forall T \in \mathcal{T}_C; \quad \text{and} \quad (5.14)$$

$$\hat{\Sigma}_{ac}(y_F; \bullet) = \Sigma_a(y_F; \bullet) \quad \forall \mathbf{F} \in \mathbb{R}^{2 \times 2}. \quad (5.15)$$

Moreover, there exists a constant \hat{L}_{ac} , which depends only on \bar{C} , such that

$$|\hat{\Sigma}_{ac}(y; T) - \hat{\Sigma}_{ac}(y_F; T)| \leq \hat{L}_{ac} M_2 \|D^2 y\|_{\ell^\infty(T \cap \mathcal{L})} \quad \forall T \in \mathcal{T}_I, \quad \mathbf{F} = \partial_T y. \quad (5.16)$$

Proof. Identity (5.12) follows from (5.2) and the fact that $\widehat{\Sigma}_{\text{ac}} - \Sigma_{\text{ac}}$ is divergence-free.

Identity (5.13) follows from (5.5) and the fact that $\widehat{\psi}^{\text{ac}}(y; m_f) = 0$ for all $f \in \mathcal{F}_{\mathcal{A}}$, which implies that $\widehat{\Sigma}_{\text{ac}}(y; T) = \Sigma_{\text{ac}}(y; T) = \Sigma_{\text{a}}(y; T)$ for all $T \in \mathcal{T}_{\mathcal{A}}$. Similarly, (5.14) follows from (5.6), and the fact that $\widehat{\psi}^{\text{ac}} = \psi^{23}$ in all elements $T \in \mathcal{T}_{\mathcal{C}}$.

Fix $\mathbf{F} \in \mathbb{R}^{2 \times 2}$. To prove (5.15) we first note that, since $\psi^{23}(y_{\mathbf{F}}; \bullet) = 0$, we have $\widehat{\psi}^{\text{ac}}(y_{\mathbf{F}}; \bullet) = \psi^{\text{ac}}(\mathbf{F}; \bullet)$. Using (5.7), we obtain

$$\widehat{\Sigma}_{\text{ac}}(y_{\mathbf{F}}; \bullet) = \Sigma_{\text{ac}}(\mathbf{F}; \bullet) - \partial \psi^{\text{ac}}(\mathbf{F}; \bullet) \mathbf{J} = \Sigma_{\text{a}}(y_{\mathbf{F}}; \bullet).$$

We are only left to prove the Lipschitz property (5.16). With $\mathbf{F} := \partial_T y$, we have

$$|\widehat{\Sigma}_{\text{ac}}(y; T) - \widehat{\Sigma}_{\text{ac}}(y_{\mathbf{F}}; T)| \leq |\Sigma_{\text{ac}}(y; T) - \Sigma_{\text{ac}}(y_{\mathbf{F}}; T)| + |\partial \widehat{\psi}^{\text{ac}}(y; T) - \partial \widehat{\psi}^{\text{ac}}(y_{\mathbf{F}}; T)|. \quad (5.17)$$

From its definition (5.3), and the fact that second partial derivatives of V are globally bounded, it is clear that Σ_{ac} satisfies a Lipschitz property of the form

$$|\Sigma_{\text{ac}}(y; T) - \Sigma_{\text{ac}}(y_{\mathbf{F}}; T)| \leq L_1 M_2 \|D^2 y\|_{\ell^\infty(T \cap \mathcal{L})} \quad (5.18)$$

where L_1 depends only on \bar{C} ; see also [9, Lemma 19] for a similar result. (If the reconstruction parameters satisfy the one-sidedness condition (3.1), as well as the patch test conditions (2.6), (2.7), one may show that $L_1 = 3\bar{C}/\Omega_0$.)

To bound the second term on the right-hand side in (5.17) we invoke the inverse inequality

$$|\partial \widehat{\psi}^{\text{ac}}(y; T) - \partial \widehat{\psi}^{\text{ac}}(y_{\mathbf{F}}; T)| \leq \frac{2}{\Omega_0} \sum_{\substack{f \in \mathcal{F} \\ f \subset T}} |\widehat{\psi}^{\text{ac}}(y; m_f) - \widehat{\psi}^{\text{ac}}(y_{\mathbf{F}}; m_f)|,$$

where we used the fact that $|\partial \zeta_f| = 2/\Omega_0$ for all $f \in \mathcal{F}$. If $f \in \mathcal{F}_{\mathcal{A}}$, then $\widehat{\psi}^{\text{ac}}(\bullet; m_f) = 0$. If $f \in \mathcal{F}_{\mathcal{C}}$, then $\widehat{\psi}^{\text{ac}}(\bullet; m_f) = \psi^{23}(\bullet; m_f)$ and hence, using (4.23),

$$|\widehat{\psi}^{\text{ac}}(y; m_f) - \widehat{\psi}^{\text{ac}}(y_{\mathbf{F}}; m_f)| = |\psi^{23}(y; m_f) - \psi^{23}(y_{\mathbf{F}}; m_f)| \leq \frac{1}{6} M_2 \|D^2 y\|_{\ell^\infty(T \cap \mathcal{L})}.$$

If $f \in \mathcal{F}_{\mathcal{I}}$, then $\widehat{\psi}^{\text{ac}}(y; m_f) = \psi^{\text{ac}}(\mathbf{F}_f; m_f)$ and $\widehat{\psi}^{\text{ac}}(y_{\mathbf{F}}; m_f) = \psi^{\text{ac}}(\mathbf{F}; m_f)$. We can therefore employ (5.9) to estimate

$$\begin{aligned} |\widehat{\psi}^{\text{ac}}(y; m_f) - \widehat{\psi}^{\text{ac}}(y_{\mathbf{F}}; m_f)| &= |\psi^{\text{ac}}(\mathbf{F}_f; m_f) - \psi^{\text{ac}}(\mathbf{F}; m_f)| \\ &\leq L_{\text{ac}} M_2 |\mathbf{F}_f - \mathbf{F}| \leq \frac{L_{\text{ac}} M_2}{2\Omega_0} \|D^2 y\|_{\ell^1(T \cap \mathcal{L})}. \end{aligned}$$

The last inequality can be verified through straightforward geometric arguments. Without explicit constants its validity is obvious.

Combining the two foregoing estimates, we obtain

$$|\partial \widehat{\psi}^{\text{ac}}(y; T) - \partial \widehat{\psi}^{\text{ac}}(y_{\mathbf{F}}; T)| \leq c \max(L_{\text{ac}}, 1) M_2 \|D^2 y\|_{\ell^\infty(\mathcal{L} \cap T)}. \quad (5.19)$$

Combining (5.17), (5.18) and (5.19), yields (5.16). \square

5.3. Proof of Theorem 5.1. With the preparations of the foregoing sections it is now easy to complete the proof of the main consistency result, Theorem 5.1. Again, we drop the dependence on y whenever possible. We begin by splitting the consistency error into a continuum

contribution and an interface contribution,

$$\begin{aligned}
\langle \delta \mathcal{E}_{\text{ac}} - \delta \mathcal{E}_{\text{a}}, u \rangle &= \sum_{T \in \mathcal{T}} |T| [\widehat{\Sigma}_{\text{ac}}(T) - \Sigma_{\text{a}}(T)] : \partial_T u \\
&= \sum_{T \in \mathcal{T}_{\text{C}}} |T| [\widehat{\Sigma}_{\text{ac}}(T) - \Sigma_{\text{a}}(T)] : \partial_T u + \sum_{T \in \mathcal{T}_{\text{I}}} |T| [\widehat{\Sigma}_{\text{ac}}(T) - \Sigma_{\text{a}}(T)] : \partial_T u \\
&=: \mathbf{E}_{\text{C}} + \mathbf{E}_{\text{I}},
\end{aligned}$$

and estimate \mathbf{E}_{C} and \mathbf{E}_{I} separately. Note also that we used (5.13) to drop the sum over elements in the atomistic region.

Using the fact that $\widehat{\Sigma}_{\text{ac}} = \Sigma_{\text{c}}^2$ in \mathcal{T}_{C} , (5.14), and the stress estimate (4.17), we obtain

$$\begin{aligned}
\mathbf{E}_{\text{C}} &\leq \sum_{T \in \mathcal{T}_{\text{C}}} |T| |\Sigma_{\text{c}}^2(T) - \Sigma_{\text{a}}(T)| |\partial_T u| \\
&\leq c \left(\sum_{x \in \mathcal{C}} [M_2 |D^3 y(x)| + M_3 |D^2 y(x)|^2]^p \right)^{1/p} \left(\sum_{T \in \mathcal{T}_{\text{C}}} |T| |\partial_T u|^{p'} \right)^{1/p'} \\
&\leq c \left(M_2 \|D^3 y\|_{\ell^p(\mathcal{C})} + M_3 \|D^2 y\|_{\ell^{2p}(\mathcal{C})}^2 \right) \left(\sum_{T \in \mathcal{T}_{\text{C}}} |T| |\partial_T u|^{p'} \right)^{1/p'}. \tag{5.20}
\end{aligned}$$

To estimate \mathbf{E}_{I} , we employ the Lipschitz property (5.16) for $\widehat{\Sigma}_{\text{ac}}$ and the fact that $\Sigma_{\text{ac}} = \Sigma_{\text{a}}$ under homogeneous deformations (see (5.15)). Using (2.8) it is also straightforward to prove

$$|\Sigma_{\text{a}}(y; T) - \Sigma_{\text{a}}(y_{\text{F}}; T)| \leq \frac{1}{\Omega_0} M_2 \|D^2 y\|_{\ell^\infty(T \cap \mathcal{L})} \quad \forall T \in \mathcal{T}, \quad \mathbf{F} = \partial_T y. \tag{5.21}$$

Using (5.15), (5.16) and (5.21), we obtain, for any $T \in \mathcal{T}_{\text{I}}$,

$$\begin{aligned}
|\widehat{\Sigma}_{\text{ac}}(y; T) - \Sigma_{\text{a}}(y; T)| &\leq |\widehat{\Sigma}_{\text{ac}}(y; T) - \widehat{\Sigma}_{\text{ac}}(y_{\text{F}}; T)| + |\Sigma_{\text{a}}(y; T) - \Sigma_{\text{a}}(y_{\text{F}}; T)| \\
&\leq \hat{L}_{\text{ac}} M_2 \|D^2 y\|_{\ell^\infty(T \cap \mathcal{L})} + \frac{1}{\Omega_0} M_2 \|D^2 y\|_{\ell^\infty(T \cap \mathcal{L})},
\end{aligned}$$

and summing over $T \in \mathcal{T}_{\text{I}}$ yields

$$\begin{aligned}
\mathbf{E}_{\text{I}} &\leq \sum_{T \in \mathcal{T}_{\text{I}}} |T| (\hat{L}_{\text{ac}} + \frac{1}{\Omega_0}) M_2 \|D^2 y\|_{\ell^\infty(T \cap \mathcal{L})} |\partial_T u| \\
&\leq c C_{\text{I}} M_2 \|D^2 y\|_{\ell^p(\mathcal{I}^{\text{ext}})} \left(\sum_{T \in \mathcal{T}_{\text{I}}} |T| |\partial_T u|^{p'} \right)^{1/p'}, \tag{5.22}
\end{aligned}$$

where C_{I} depends only on \hat{L}_{ac} , which depends only on \bar{C} .

Combining (5.22) and (5.20) we finally obtain the desired consistency error estimate (5.1). This concludes the proof of Theorem 5.1.

6. APPENDIX: PROOF OF LEMMA 5.2 (II)

In this appendix, we provide the remaining details for the proof of Lemma 5.2 (ii). Throughout this proof we fix a homogeneous deformation y_{F} , $\mathbf{F} \in \mathbb{R}^{2 \times 2}$, and drop the argument $y = y_{\text{F}}$ whenever possible. For example, we will write $\Sigma_{\text{ac}}(T) = \Sigma_{\text{ac}}(y_{\text{F}}; T)$.

We begin by computing an expression for $\Sigma_{\text{ac}} - \Sigma_{\text{a}}$ in terms of the parameters $C_{x,j}$. Equation (3.8), in the proof of Lemma 3.2, can be rewritten in the form

$$V_{x, \mathbf{F}, j}^{\text{ac}} := \partial_j V_x^{\text{ac}}(\mathbf{F}\mathbf{a}) = (1 - C_{x, j-1}) V_{\mathbf{F}, j-1} + C_{x, j} V_{\mathbf{F}, j} + (1 - C_{x, j+1}) V_{\mathbf{F}, j+1}.$$

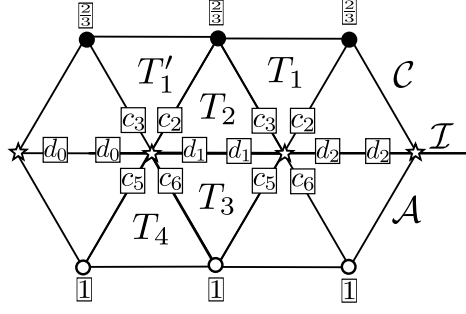


FIGURE 7. Visualisation of the flat interface analysis in §6.1.

Recalling also (4.12) and using $a_j = a_{j-1} + a_{j+1}$, we obtain

$$\begin{aligned}
\Sigma_{ac}(T) - \Sigma_a(T) &= \sum_{j=1}^6 [V_{x_{T,j},F,j}^{ac} - V_{F,j}] \otimes a_j \\
&= \frac{1}{\Omega_0} \sum_{j=1}^6 [(1 - C_{x_{T,j},j-1})V_{F,j-1} + (C_{x_{T,j},j} - 1)V_{F,j} + (1 - C_{x_{T,j},j+1})V_{F,j+1}] \otimes a_j \\
&= \frac{1}{\Omega_0} \sum_{j=1}^6 V_{F,j} \otimes [(1 - C_{x_{T,j-1},j})a_{j-1} + (C_{x_{T,j},j} - 1)a_j + (1 - C_{x_{T,j+1},j})a_{j+1}] \\
&= \frac{1}{\Omega_0} \sum_{j=1}^6 V_{F,j} \otimes [-C_{x_{T,j-1},j}a_{j-1} + C_{x_{T,j},j}a_j - C_{x_{T,j+1},j}a_{j+1}]. \tag{6.1}
\end{aligned}$$

The explicit evaluation of (6.1) for interface elements is carried out separately for flat interfaces and interfaces with corners.

For triangles not intersecting the interface, $\Sigma_{ac}(y_F; T) - \Sigma_a(y_F; T) = 0$, hence we need to compute the stress errors only for interface elements.

6.1. Flat interface. Consider the flat interface configuration in Figure 7. According to (3.10) and (3.11) the free parameters are $c_j := C_{x,j}$ (for $x \in \mathcal{I}$ and $j \in \{2, 3, 5, 6\}$), and $d_i, i \in \mathbb{Z}$, where $d_1 = C_{x_{T_2,1,1}} = C_{x_{T_2,4,4}}$, and so forth. We calculate the a/c stress for the elements T_1, T_2 , and collect the results in Table 1.

From Table 1 we can read off the stress differences $\Sigma_{ac} - \Sigma_a$ in the elements T_1, T_2 :

$$\begin{aligned}
\Sigma_{ac}(T_1) - \Sigma_a(T_1) &= \left\{ \left(\frac{2}{3} - d_2\right)V_{F,1} + (c_2 - \frac{2}{3})V_{F,2} + \left(\frac{2}{3} - c_3\right)V_{F,3} \right\} \otimes \frac{a_2}{\Omega_0} \\
&\quad + \left\{ \left(d_1 - \frac{2}{3}\right)V_{F,1} + \left(\frac{2}{3} - c_2\right)V_{F,2} + \left(c_3 - \frac{2}{3}\right)V_{F,3} \right\} \otimes \frac{a_3}{\Omega_0},
\end{aligned}$$

TABLE 1. Table of coefficients of $V_{F,j}$ in (6.1), in interfacial triangles, on flat interfaces.

	j	$C_{x_{T,j-1},j}$	$C_{x_{T,j},j}$	$C_{x_{T,j+1},j}$	$-C_{x_{T,j-1},j}a_{j-1} + C_{x_{T,j},j}a_j - C_{x_{T,j+1},j}a_{j+1}$
T_1	1	$\frac{2}{3}$	$\frac{2}{3}$	d_2	$-\frac{2}{3}a_6 + \frac{2}{3}a_1 - d_2a_2 = (\frac{2}{3} - d_2)a_2$
	2	$\frac{2}{3}$	c_2	c_2	$-\frac{2}{3}a_1 + c_2a_2 - c_2a_3 = (-\frac{2}{3} + c_2)(a_2 - a_3)$
	3	c_3	c_3	$\frac{2}{3}$	$-c_3a_2 + c_3a_3 - \frac{2}{3}a_4 = (\frac{2}{3} - c_3)(a_2 - a_3)$
	4	d_1	$\frac{2}{3}$	$\frac{2}{3}$	$-d_1a_3 + \frac{2}{3}a_4 - \frac{2}{3}a_5 = (\frac{2}{3} - d_1)a_3$
	5	$\frac{2}{3}$	$\frac{2}{3}$	$\frac{2}{3}$	0
	6	$\frac{2}{3}$	$\frac{2}{3}$	$\frac{2}{3}$	0
T_2	1	$\frac{2}{3}$	d_1	d_1	$-\frac{2}{3}a_6 + d_1a_1 - d_1a_2 = (\frac{2}{3} - d_1)a_3$
	2	c_2	c_2	c_2	0
	3	c_3	c_3	c_3	0
	4	d_1	d_1	$\frac{2}{3}$	$-d_1a_3 + d_1a_4 - \frac{2}{3}a_5 = (\frac{2}{3} - d_1)a_2$
	5	c_5	$\frac{2}{3}$	$\frac{2}{3}$	$-c_5a_4 + \frac{2}{3}a_5 - \frac{2}{3}a_6 = (c_5 - \frac{2}{3})a_1$
	6	$\frac{2}{3}$	$\frac{2}{3}$	c_6	$-\frac{2}{3}a_5 + \frac{2}{3}a_6 - c_6a_1 = (\frac{2}{3} - c_6)a_1$

and

$$\begin{aligned}
\Sigma_{\text{ac}}(T_2) - \Sigma_{\text{a}}(T_2) &= \left\{ (d_1 - \frac{2}{3})V_{F,1} + (\frac{2}{3} - c_5)V_{F,2} + (c_6 - \frac{2}{3})V_{F,3} \right\} \otimes \frac{a_1}{\Omega_0} \\
&= \left\{ (d_1 - \frac{2}{3})V_{F,1} + (\frac{2}{3} - c_2)V_{F,2} + (c_3 - \frac{2}{3})V_{F,3} \right\} \otimes \frac{a_2}{\Omega_0} \\
&\quad - \left\{ (d_1 - \frac{2}{3})V_{F,1} + (\frac{2}{3} - c_2)V_{F,2} + (c_3 - \frac{2}{3})V_{F,3} \right\} \otimes \frac{a_3}{\Omega_0} \\
&\quad + \left\{ (c_2 - c_5)V_{F,2} + (c_6 - c_3)V_{F,3} \right\} \otimes \frac{a_1}{\Omega_0}.
\end{aligned}$$

Note that we have provided two alternative representations of $\Sigma_{\text{ac}}(T_2) - \Sigma_{\text{a}}(T_2)$, since the first representation is in general insufficient to construct the corrector.

Since the atomistic region is a mirror image of the continuum region with respect to the interface, we can obtain stress function $\Sigma_{\text{ac}}(y_{\text{F}}; \cdot)$ for T_3 and T_4 from symmetry considerations:

$$\begin{aligned}
\Sigma_{\text{ac}}(T_4) - \Sigma_{\text{a}}(T_4) &= \left\{ (1 - d_0)V_{F,1} + (c_5 - 1)V_{F,2} + (1 - c_6)V_{F,3} \right\} \otimes \frac{a_2}{\Omega_0} \\
&\quad + \left\{ (d_1 - 1)V_{F,1} + (1 - c_5)V_{F,2} + (c_6 - 1)V_{F,3} \right\} \otimes \frac{a_3}{\Omega_0},
\end{aligned}$$

and

$$\begin{aligned}
\Sigma_{\text{ac}}(T_3) - \Sigma_{\text{a}}(T_3) &= \left\{ (d_1 - 1)V_{F,1} + (1 - c_2)V_{F,2} + (c_3 - 1)V_{F,3} \right\} \otimes \frac{a_1}{\Omega_0} \\
&= \left\{ (d_1 - 1)V_{F,1} + (1 - c_5)V_{F,2} + (c_6 - 1)V_{F,3} \right\} \otimes \frac{a_2}{\Omega_0} \\
&\quad - \left\{ (d_1 - 1)V_{F,1} + (1 - c_5)V_{F,2} + (c_6 - 1)V_{F,3} \right\} \otimes \frac{a_3}{\Omega_0} \\
&\quad - \left\{ (c_2 - c_5)V_{F,2} + (c_6 - c_3)V_{F,3} \right\} \otimes \frac{a_1}{\Omega_0}.
\end{aligned}$$

From the proof Lemma 4.5 recall that $\partial\zeta_f(T)\mathbf{J} = -\frac{2}{\Omega_0}a_j$ if f is an edge of T and a_j the counter-clockwise direction of the edge (relative to T). We can therefore choose ψ^{ac} explicitly, for example, for $f = T_1 \cap T_2$:

$$\psi^{\text{ac}}(\mathbf{F}; m_f) := \frac{1}{2} \left\{ (d_1 - \frac{2}{3})V_{F,1} + (\frac{2}{3} - c_2)V_{F,2} + (c_3 - \frac{2}{3})V_{F,3} \right\}. \quad (6.2)$$

For the remaining edges, similar choices can be made, the crucial observation being that the terms in neighbouring elements associated with an edge cancel each other out.

We observe, moreover, that for the triangles T_1 and T_4 , the a_1 components of the stresses vanish, which means that $\psi^{\text{ac}}(\mathbf{F}; m_f) = 0$ for all $f \in \mathcal{F}_{\mathcal{A}} \cup \mathcal{F}_{\mathcal{C}}$. This proves (5.8) in the flat interface case.

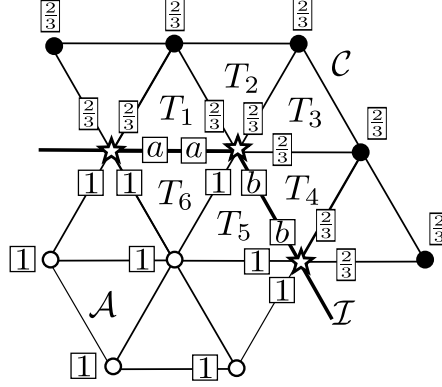


FIGURE 8. Interface configuration with corner.

It remains to prove the Lipschitz bound (5.9). From (6.2) (and the corresponding formulas for the remaining edges), it is straightforward to show that ψ^{ac} is Lipschitz continuous for any fixed set of parameters with a Lipschitz constant of the form LM_2 , where L can be bounded in terms of \bar{C} . This concludes the proof of Lemma 5.2 (ii) in the flat interface case.

Remark 6.1 (Correctors are necessary). From the calculation in this section, it is clear that one cannot choose parameters such that $\Sigma_{\text{ac}}(y_{\text{F}}; T) = \Sigma_{\text{a}}(y_{\text{F}}; T)$ for all $T \in \mathcal{T}$ and for all potentials $V \in \mathcal{V}$. For example, if $\Sigma_{\text{ac}}(y_{\text{F}}; T_2) = \Sigma_{\text{a}}(y_{\text{F}}; T_2)$ for all V , then $d_1 = 2/3$, whereas if $\Sigma_{\text{ac}}(y_{\text{F}}; T_3) = \Sigma_{\text{a}}(y_{\text{F}}; T_3)$, then $d_1 = 1$. This demonstrates that the divergence-free corrector fields are in fact necessary, and that it is impossible in our current framework to construct an a/c method where $\Sigma_{\text{ac}}(y_{\text{F}}; T) = \Sigma_{\text{a}}(y_{\text{F}}; T)$ holds for all $T \in \mathcal{T}, \mathbf{F} \in \mathbb{R}^{2 \times 2}$, and $V \in \mathcal{V}$. \square

6.2. General interface. We now turn to the proof of (5.7)–(5.9) for interface configurations with corners. Consider the corner configuration displayed in Figure 8, which is concave from the point of view of the atomistic region. The reconstruction coefficients found in Proposition 3.6 are displayed in the figure as well. Recall that the reconstructions of bonds into the atomistic or continuum regions are now uniquely determined, while the bonds lying at the interfaces (parameters a and b) are still free.

Using (6.1), and defining $a'_j := a_j/\Omega_0$, the stress errors $\Sigma_{\text{ac}} - \Sigma_{\text{a}}$ in the elements T_1, \dots, T_6 can again be computed explicitly:

$$\begin{aligned} \Sigma_{\text{ac}}(T_1) - \Sigma_{\text{a}}(T_1) &= \left(\frac{1}{3}V_{\text{F},3} - \frac{1}{3}V_{\text{F},2}\right) \otimes a'_1 + \left(a - \frac{2}{3}\right)V_{\text{F},1} \otimes a'_2 - \left(a - \frac{2}{3}\right)V_{\text{F},1} \otimes a'_3, \\ \Sigma_{\text{ac}}(T_2) - \Sigma_{\text{a}}(T_2) &= \left(a - \frac{2}{3}\right)V_{\text{F},1} \otimes a'_3, \\ \Sigma_{\text{ac}}(T_3) - \Sigma_{\text{a}}(T_3) &= \left(b - \frac{2}{3}\right)V_{\text{F},3} \otimes a'_1, \\ \Sigma_{\text{ac}}(T_4) - \Sigma_{\text{a}}(T_4) &= -\left(b - \frac{2}{3}\right)V_{\text{F},3} \otimes a'_1 + \left(b - \frac{2}{3}\right)V_{\text{F},3} \otimes a'_2 + \left(\frac{1}{3}V_{\text{F},1} - \frac{1}{3}V_{\text{F},2}\right) \otimes a'_3, \\ \Sigma_{\text{ac}}(T_5) - \Sigma_{\text{a}}(T_5) &= \left(\frac{1}{3}V_{\text{F},2} - \frac{1}{3}V_{\text{F},1}\right) \otimes a'_3 + \left[(1-a)V_{\text{F},1} + (b-1)V_{\text{F},3}\right] \otimes a'_2 \\ &\quad - (b-1)V_{\text{F},3} \otimes a'_1, \quad \text{and} \\ \Sigma_{\text{ac}}(T_6) - \Sigma_{\text{a}}(T_6) &= \left(\frac{1}{3}V_{\text{F},2} - \frac{1}{3}V_{\text{F},3}\right) \otimes a'_1 + \left[(a-1)V_{\text{F},1} + (1-b)V_{\text{F},3}\right] \otimes a'_2 \\ &\quad - (a-1)V_{\text{F},1} \otimes a'_3. \end{aligned}$$

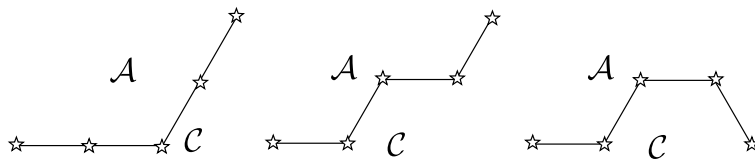


FIGURE 9. All possible corner configurations (up to translation, rotation and reflection).

Following the argument in §6.1, we can check again that the associated edge contributions from neighbouring elements cancel, and hence we can explicitly construct the corrector function ψ^{ac} . Note that $\Sigma_{ac}(T_2)$ has no a'_1 component and $\Sigma_{ac}(T_5)$ has no a'_3 component, which implies (5.8).

For a corner that is convex from the point of view of the atomistic region, the result follows by symmetry (interchanging the coefficients 1 and $\frac{2}{3}$). The Lipschitz bound (5.9) can be obtained from the above formulas, under the assumption that the reconstruction coefficients a, b are bounded above by \bar{C} .

Finally, we have to convince ourselves that our above argument applies to all possible interface geometries. In Figure 9 we present an exhaustive list, up to translations, rotations and reflections, of local interface geometries. (Recall our geometric requirements formulated in Assumption 3.5.) By inspecting the calculation of the stress differences $\Sigma_{ac} - \Sigma_a$ for the case presented in Figure 8, one observes that the formulas are local, and do not depend on the extended geometry of the interface. We note, however, that this only holds due to the separation Assumption 3.5. The subsequent construction of the corrector now follow of course verbatim.

This concludes the proof of Lemma 5.2 (ii) in the general interface case.

7. CONCLUSION

We have shown for a 2D model problem that it is possible to construct patch test consistent a/c coupling method for multi-body potentials, in interface geometries with corners, using a new variant of the geometry reconstruction technique introduced in [3, 17], which we labelled the GR-AC method. Moreover, we have proven a quasi-optimal consistency error estimate for the GR-AC method(s) we constructed.

We see this work as a first step towards a general theory of GR-AC method(s). Our goal is to show eventually that the free parameters in the method can *always* (that is, in any dimension, for any interface geometry) be determined so as to satisfy the energy and force consistency conditions, and that the resulting GR-AC method(s) will have the same consistency properties that we establish in the present case.

An important issue that we have left entirely open in the present work is the stability of the GR-AC method: Under which conditions on the reconstruction parameters does the GR-AC method have sharp stability properties as discussed in [2]? This issue is the topic of ongoing research.

REFERENCES

- [1] M. Dobson and M. Luskin. An optimal order error analysis of the one-dimensional quasicontinuum approximation. *SIAM Journal on Numerical Analysis*, 47(4):2455–2475, 2009.
- [2] M. Dobson, M. Luskin, and C. Ortner. Accuracy of quasicontinuum approximations near instabilities. *J. Mech. Phys. Solids.*, 58(10):1741–1757, 2010.

- [3] W. E, J. Lu, and J.Z. Yang. Uniform accuracy of the quasicontinuum method. *Phys. Rev. B*, 74(21):214115, 2006.
- [4] W. E and P. Ming. Cauchy-Born rule and the stability of crystalline solids: static problems. *Arch. Ration. Mech. Anal.*, 183(2):241–297, 2007.
- [5] J. Lu and P. Ming. Convergence of a force-based hybrid method for atomistic and continuum models in three dimensions. arXiv:1102.2523v2.
- [6] R. Miller and E. Tadmor. A unified framework and performance benchmark of fourteen multiscale atomistic/continuum coupling methods. *Modelling Simul. Mater. Sci. Eng.*, 17, 2009.
- [7] P. Ming and J. Z. Yang. Analysis of a one-dimensional nonlocal quasi-continuum method. *Multiscale Modeling & Simulation*, 7(4):1838–1875, 2009.
- [8] M. Ortiz, R. Phillips, and E. B. Tadmor. Quasicontinuum analysis of defects in solids. *Philosophical Magazine A*, 73(6):1529–1563, 1996.
- [9] C. Ortner. The role of the patch test in 2d atomistic-to-continuum coupling methods. arXiv:1101.5256.
- [10] C. Ortner. A priori and a posteriori analysis of the quasi-nonlocal quasicontinuum method in 1d. *Math. Comp.*, 80:1265–1285, 2011.
- [11] C. Ortner and A. V. Shapeev. Analysis of an energy-based atomistic/continuum coupling approximation of a vacancy in the 2d triangular lattice. arXiv:1104.0311.
- [12] C. Ortner and H. Wang. Coarse graining in energy-based quasicontinuum methods. To appear in *Math. Models Meth. Appl. Sc.*
- [13] K. Polthier and E. Preuss. identifying vector field singularities using a discrete hodge decomposition. In *Visualization and Mathematics III*. Springer Verlag, 2002.
- [14] A. Shapeev. Consistent energy-based atomistic/continuum coupling for two-body potentials in three dimensions. arXiv:1108.2991.
- [15] A. V. Shapeev. Consistent energy-based atomistic/continuum coupling for two-body potentials in one and two dimensions. *Multiscale Model. Simul.*, 9:905–932, 2011.
- [16] V. B. Shenoy, R. Miller, E. B. Tadmor, D. Rodney, R. Phillips, and M. Ortiz. An adaptive finite element approach to atomic-scale mechanics—the quasicontinuum method. *J. Mech. Phys. Solids*, 47(3):611–642, 1999.
- [17] T. Shimokawa, J.J. Mortensen, J. Schiotz, and K.W. Jacobsen. Matching conditions in the quasicontinuum method: Removal of the error introduced at the interface between the coarse-grained and fully atomistic region. *Phys. Rev. B*, 69(21):214104, 2004.

C. ORTNER, MATHEMATICS INSTITUTE, ZEEMAN BUILDING, UNIVERSITY OF WARWICK, COVENTRY CV4 7AL, UK

E-mail address: c.ortner@warwick.ac.uk

L. ZHANG, MATHEMATICAL INSTITUTE, 24-29 ST GILES’, OXFORD OX1 3LB, UK

E-mail address: zhang@maths.ox.ac.uk